Endocytic Sorting and Downregulation of the M2 Acetylcholine Receptor is Regulated by Ubiquitin and the ESCRT Complex

Dmitry Zenko[1,2], Dawn Thompson[1] and James N Hislop[1]*

[1]Institute of Medical Sciences, School of Medicine, Medical Sciences and Nutrition, University of Aberdeen, AB25 2ZD.

[2]Current Address – Nuffield Department of Clinical Neurosciences, University of Oxford, Medical Sciences Division, OX3 9DU

*To whom correspondence should be addressed: james.hislop@abdn.ac.uk

Running Title - M2R Downregulation

Highlights

- M2 muscarinic acetylcholine receptors undergo rapid and extensive agonist-induced proteolysis
- M2R downregulation is predominantly in the lysosome and is regulated by direct receptor ubiquitination and the associated ESCRT machinery
- Ubiquitin is the prime regulator of endocytic sorting and its disruption leads to increased receptor recycling.

Keywords:

Muscarinic Receptor, lysosome, ubiquitin, endosome, ESCRT, recycling

Abstract

Cholinergic dysfunction plays a critical role in a number of disease states, and the loss of functional muscarinic acetylcholine receptors plays a key role in disease pathogenesis. Therefore, preventing receptor downregulation would maintain functional receptor number, and be predicted to alleviate symptoms. However, the molecular mechanism(s) underlying muscarinic receptor downregulation are currently unknown. Here we demonstrate that the M2 muscarinic receptor undergoes rapid lysosomal proteolysis, and this lysosomal trafficking is facilitated by ubiquitination of the receptor. Importantly, we show that this trafficking is driven specifically by ESCRT mediated involution. Critically, we provide evidence that disruption of this process leads to a re-routing of the trafficking of the M2 receptor away from the lysosome and into recycling pathway, and eventually back to the plasma membrane. This study is the first to identify the process by which the M2 muscarinic receptor undergoes endocytic sorting, and critically reveals a regulatory checkpoint that represents a target to pharmacologically increase the number of functional muscarinic receptors within the central nervous system.

1. Introduction

Cholinergic dysfunction is critical in the pathophysiology of various disorders including Alzheimer's, Parkinson's, schizophrenia and addiction, and, an understanding into how the cholinergic system is regulated, is of vital importance for the identification of therapeutic targets (Felder et al., 2000; Langmead et al., 2008; McKinzie and Bymaster, 2012; Wess et al., 2007). Central to the regulation of the cholinergic system are the muscarinic family of acetylcholine receptors (mAChRs[1]), M1-5, the activation of which plays a critical modulatory role within the central nervous system (CNS) (Lebois et al., 2018; Levey, 1996). Disruption of mAChR function can result in range of pathophysiological effects, both peripherally and within the CNS (Kruse et al., 2014; Thomsen et al., 2018; Wess et al., 2007). Accordingly, a reduction in functional mAChR receptor number has been observed in patients with Alzheimer's disease, bipolar disorder, schizophrenia and psychosis (Gibbons et al., 2016, 2013; Scarr, 2012; Scarr et al., 2018). Despite its undoubted importance, little is known regarding the mechanisms regulating the receptor number of mAChR.

All five mAChRs belong to the G-protein-coupled receptor (GPCR) family of membrane proteins (Kruse et al., 2014; Lebois et al., 2018). One important mechanism by which the levels of functional GPCR are maintained is by endocytic trafficking, and the sorting of these receptors to the lysosome for proteolysis and downregulation, preventing overstimulation. It is now well established that mAChRs, like other GPCRs, undergo extensive endocytic trafficking followed by downregulation in the face of excess activation (Bernard et al., 2003, 1999; Decossas et al., 2005; Thangaraju and Sawyer, 2011), however, the molecular mechanisms responsible for this process remain broadly unknown (Reiner and Nathanson, 2012; Zenko and Hislop, 2018).

The established model for the regulation of GPCRs involves agonist activated receptors first being uncoupled from the G-protein (desensitization) by a combination of phosphorylation (mediated by G-protein Receptor kinases) and interaction with

[1] **Abbreviations:** AlexFluor – AF, CNS – Central Nervous System, DRG - Dorsal Root Ganglia, EEA1 - Early Endosome Antigen 1, ESCRT - Endosomal Sorting Complex Required for Transport, GPCR - G-Protein-Coupled-Receptor, HEK 293 - Human Embryonic Kidney 293 cell line, LAMP1 - lysosomal associated membrane protein 1, M2R - muscarinic receptor 2, mAChR - muscarinic acetylcholine receptor, MVB - Multivesicular Body, PAR - Protease activated receptor, QNB - quinuclidinyl benzilate

arrestins (Ferguson, 2001; Krupnick and Benovic, 1998; Pierce et al., 2001). Desensitized receptors are then removed from the plasma membrane to prevent further activation by ligands (Hanyaloglu and von Zastrow, 2008; Sorkin and Von Zastrow, 2002). Following internalization into the endocytic pathway, GPCRs, like other membrane cargo, can either undergo recycling back to the plasma membrane leading to functional resensitization, or are transported to the lysosome for proteolysis and long-term downregulation (Eden et al., 2012; Hanyaloglu and von Zastrow, 2008; Hislop and von Zastrow, 2011; Zenko and Hislop, 2018). Central to lysosomal targeting is the regulatory protein ubiquitin. Sorting of membrane cargo including the GPCR Ste2p (Hicke and Riezman, 1996) to the lysosome/vacuole has been extensively studied in the yeast model system, and also in mammalian cells (Dunn and Hicke, 2001; Haglund and Dikic, 2012; Wendland et al., 1998). The covalent attachment of ubiquitin and polyubiquitin chains to the cytoplasmic portion of membrane proteins, such as the epidermal growth factor receptor (EGFR), prevents recycling and targets the receptor to the lumen of the endosome by a process termed involution (Katzmann et al., 2002; Raiborg and Stenmark, 2009; Saksena et al., 2007; Schoneberg et al., 2017). These larger, more spherical endosomes, known as multivesicular bodies, have a number of receptor containing intraluminal vesicles that can now be exposed to lipases and proteases upon fusion with the lysosome leading to proteolysis and long term downregulation of the receptor. Involution and lysosomal sorting are driven by the interaction of the ubiquitinated cargo with a complex of proteins collectively known as the Endosomal Sorting Complex Required for Sorting (ESCRT), thus ubiquitin regulates both the sorting and subsequent proteolysis of these membrane receptors (Katzmann et al., 2002; Raiborg et al., 2003; Razi and Futter, 2006). For GPCRs, however, the role of ubiquitination is far less clear, with some receptors requiring ubiquitination, some having no requirement for ubiquitination, and other GPCRs utilising ubiquitin for proteolysis, but not for actively sorting the receptor to the lysosome. (Hislop and von Zastrow, 2011; Marchese and Trejo, 2013; Skieterska et al., 2017). Importantly, the role of ubiquitination and the mechanism(s) responsible for lysosomal sorting of the mAChR has not been investigated

Although the early endocytic events have been previously investigated for the muscarinic receptors (Gurevich et al., 1995; Hosey et al., 1999; Pals-Rylaarsdam et al., 1997; Schlador and Nathanson, 1997; van Koppen, 2001), the post-endocytic fate

of this important group of receptors has been largely overlooked. Here we investigated the mechanisms responsible for the post-endocytic sorting and downregulation of a typical mAChR, the M2 mAChR (M2R), whose downregulation is physiologically relevant. Using a number of complimentary biochemical and imaging techniques, we clearly show that both receptor ubiquitination and the ESCRT machinery are required for M2R downregulation. Importantly, we also demonstrate that, in contrast to a number of GPCRs, direct ubiquitination is also the prime mechanism for sorting the M2R to the lysosome, and preventing recycling. The identification of the molecular checkpoint responsible for regulating surface receptor number of M2R represents an important target for the development of therapeutics designed to increase receptor expression and function.

2. Methods

2.1 Antibodies and Reagents

Functionally verified siRNA oligos were purchased from Qiagen (AllStars Negative Control, HRS (Hs_HGS_6 Flexitube siRNA), Tsg101 (Hs_TSG101_7 Flexitube siRNA), antibody against Flag (M1 clone) was purchased from Sigma and labelled with AlexaFluor (AF) 488, 568 or 647 fluorophores using AlexaFluor antibody labelling kit according to manufacturer's instructions (ThermoFisher).

2.2 Cell Culture, Constructs and Transfection

DNA of the coding region of the M2 muscarinic receptor (M2R) was purchased from Missouri S&T cDNA resource centre. The M2R-0cK (M2R with all intracellular lysine residues mutated to arginine) was synthesised by GeneArt (ThermoFisher). All constructs were amplified by PCR and ligated into N terminally tagged SS-Flag and SS-HA vectors (a gift from Prof. Mark von Zastrow, University of California, San Francisco UCSF)). For expression in dorsal root ganglion neurons (DRGs), PCR was used to amplify the SSF-M2R and SSF-M2R-0cK and subcloned into pCAGGS neuronal expression vector (a gift from Prof. Mark von Zastrow, UCSF (Kotowski et al., 2011)). To tag receptors in-frame with superecliptic GFP, cDNA of SSF-M2 and SSF-M2-0cK were amplified by PCR to remove the stop codon and add an AgeI restriction site. PCR products were then subcloned into the previously described vector (Henry et al., 2011). LAMP1-RFP was a gift from Walther Mothes (Addgene plasmid #1817; http://n2t.net/addgene:1817 ; RRID:Addgene_1817 (Sherer et al.,

2003)), EGFP-β-Arr1, EGFP-β-Arr2, and EGFP-RAB5 were kind gifts from Prof. Mark von Zastrow, UCSF. EGFP-Rab11 and EGFP Rab7 was a kind gift from Dr. Rey Carabeo (Washington State University).

Human embryonic 293 (HEK 293) cells were cultured in Dubecco's modified eagle medium (DMEM) supplemented with 10% heat inactivated foetal bovine serum (FBS) and routinely passaged by lifting in PBS-EDTA. All transfections were carried out using Lipofectamine 2000 according to manufacturer instructions, unless otherwise stated. Cells were transfected in 6-well plates and then replated onto poly-L-lysine coated glass coverslips. Transfection of RNAi was achieved by the use of Lipofectamine RNAiMax according to manufacturer instructions as previously described (Hislop et al., 2009). HEK 293 cells stably expressing Flag-epitope tagged receptors were created by transfection of cDNA and selection in zeocin. Clones were screened for stable expression by immunofluorescent staining and Western Blotting.

2.3 Calcium phosphate transfection for detection of ubiquitin.

For ubiquitination assay, M2R or M2R-0cK HEK 293 cells were grown to ~50% confluency in 60mm dishes and transfected using a calcium phosphate transfection method. For each plate, 1 μg of HA-ubiquitin was dissolved in 300 μl of 25 mM $CaCl_2$. The DNA:$CaCl_2$ solution was then added dropwise (while slowly mixing to ensure precipitate formation) to an equal volume (300 μl) of 2 x HBS buffer (50 mM HEPES, 280 mM NaCl, 1.5 mM Na_2HPO_4, pH 7.0), mixed and incubated at room temperature for 30 minutes to allow precipitation. The mixture was then added dropwise to the dishes and incubated for 48 hours before experimentation.

2.4 Culture and transfection of dorsal root ganglia

All animal procedures were approved by the local Ethics Committee and performed in accordance with the United Kingdom Animals Scientific Procedures Act (1986) and associated guidelines.

DRG neurons were obtained from postnatal (P1-P2) Sprague-Dawley (SD) rats. Following schedule 1 (cervical dislocation followed by decapitation) spinal cords were carefully removed, cut through the vertebral column and DRGs were isolated one at a time using fine forceps. DRGs were incubated in the 0.025% trypsin/EDTA (Sigma-

Aldrich) for 20 minutes at 37°C following mechanic dissociation of the ganglia by triturating using a 1ml glass fire-polished pipette.

The cell suspension was then passed through a cell strainer (Cole-Parmer), collected into 50 mL centrifuge tube followed by centrifugation at 500 x g for 5 minutes. Cells were resuspended in pre-warmed neurobasal medium (Gibco) supplemented with B27 (Gibco), 1% penicillin-streptomycin (Sigma-Aldrich), 5.0 µg/mL insulin from bovine pancreas powder (Sigma-Aldrich), 1% GlutaMax (Gibco) and 50 ng/mL β-NGF (BD Biosciences). DRG neurons were then plated (70,000 cells/well) onto poly-L-lysine- and 20 ng/mL laminin- coated 12 mm coverslips and maintained for one week with half-volume of the media being replaced every 2 days.

For transfections, cells were centrifuged at 500 x g for 5 minutes and resuspended in pre-equilibrated room temperature Nucleofector® solution (100 µL per 2 x 10^6 cells per transfection), combined with 2 µg of plasmid DNA (M2R:pCAGGS or M2R-0cK:pCAGGS) and electroporated (Nucleofector II, program G-013, Amaxa Lonza). Cells were immediately placed into pre-warmed HBSS for 10 minutes before resuspension in Neurobasal media and plated onto coverslips as described above.

2.5 Biochemical detection of receptor proteolysis and protein levels by immunoblotting

Total cellular levels of protein were determined by immunoblotting as previously described (Hislop et al., 2004). Briefly, cells were plated into 12-well culture plates and treated as described in figure legends before washing in ice-cold PBS and lysing in extraction buffer (0.5% Triton X-100, 150 mM NaCl, 25 mM KCl, 25 mM Tris pH 7.4, 1 mM EDTA) supplemented with a standard protease inhibitor cocktail (Roche). Lysates were clarified by centrifugation and resolved by SDS-PAGE using an 8% acrylamide gel and transferred to nitrocellulose and detected using horseradish peroxidase-conjugated sheep anti-mouse IgG (Amersham Biosciences) or donkey anti-rabbit IgG (Sigma) and enhanced chemiluminesence (ECL) prime detection reagent (Amersham). Band intensities of unsaturated immunoblots were analysed using Peqlab software and quantified by densitometry on ImageJ.

2.6 Biotin Protection Degradation Assay

The fate of the surface, mature pool of receptors was determined by surface biotinylation as previously described (Thompson et al., 2014). Cells plated in 60mm

dishes were labelled for 30 mins at 4°C with 30 µg/ml disulfide-cleavable biotin (ThermoPierce), washed in Tris Buffered saline (TBS) and all but the 100% and strip plates (which were kept at 4°C until the end of the experiment) were incubated in 5 ml culture medium at 37°C for 15 mins before stimulation with 10 µM carbachol for 30, 90, or 180 min. Subsequently, all plates (except the 100%) were then washed (2 x PBS), stripped to remove remaining surface-biotin (50 µM glutathione, 0.3 mM NaCl, 75 mM NaOH, 1% FBS, 2 x 10 min, 4°C), quenched (PBS containing 1 mM iodoacetamide, 0.1% BSA, 10 min, 4°C), and then lysed in immunoprecipitation buffer (150 mM NaCl, 25 mM KCl, 10 mM Tris-HCl, pH 7.4, 0.1% Triton X-100, and protease inhibitors). Lysates were immunoprecipitated (anti-FLAG M2) overnight and incubated for 2 h with recombinant protein G-Sepharose (Life Technologies) and deglycosylated using PNGaseF. Samples were then resolved by SDS-PAGE and visualised with streptavidin overlay (VECTASTAIN ABC immunoperoxidase reagent, Vector Laboratories).

2.7 Receptor downregulation by radioligand binding

Receptor down-regulation was determined by radioligand binding as previously described (Thangaraju and Sawyer, 2011). HEK 293 cells stably expressing FLAG-tagged receptors were re-plated into 12-well plates. 24 h later 10 µM Carbachol was added to the cells for the indicated time period, cells were washed twice with ice-cold PBS, and 300 µl of PBS was added to the cells, and the plates were frozen. Plates were thawed, and cells passed through a 22G needle. Binding assays were performed in triplicate in 96-well plates with 15 nM [^{3}H] quinuclidinyl benzilate (QNB) (Perkin Elmer, 32.9 Ci/mmol), incubated for 3 h at 4°C. Incubations were terminated by vacuum filtration through glass fiber filters (Whatman), and repeated washes with TBS. Bound radioactivity was determined by liquid scintillation counting of washed filters. Nonspecific binding, determined by carrying out parallel determinations in the presence of excess unlabeled competitive antagonist (10 µM atropine), was <10% of specific activity added.

2.8 Live Cell Imaging using the pH-sensitive GFP variant

Involution was determined by live imaging of C-terminal tagged pH-sensitive GFP as previously described (Henry et al., 2011). Briefly, HEK 293 cells were transiently-transfected with the constitutively active mCherry-Rab5-Q79L and the indicated N-

terminally FLAG-tagged, C-terminally ecliptic GFP variant-tagged receptor constructs and plated onto polylysine-coated glass coverslips. Cells were incubated in the presence of 10 μM Carbachol for 90 min prior to imaging. Cells were imaged with an Ultra VIEW VoX spinning disc confocal microscope (Perkin Elmer) for 30s and then 500 μM chloroquine was added to cells while image acquisition continued for an additional 5 minutes with one frame taken every 5 seconds. Cross-sections showing chloroquine-induced appearance inside endosomal lumen were analysed using Volocity software. Raw data was exported to TIFF (16-bit) format and mean fluorescence intensities of individual endosomes before and after chloroquine treatment were measured using ImageJ software. Briefly, selections were drawn around each endosome and the mean fluorescence values were background corrected. Background subtracted fluorescence intensities obtained from first ten frames of image sequence were averaged and identified as the “minimum fluorescence value”. The maximum average fluorescence value was determined from the last ten frames of the acquired image sequence. The fold increase for each endosome was determined from the average maximum fluorescence value was divided by the average minimum fluorescence value.

2.9 Laser-scanning confocal microscopy of fixed specimens

HEK 293 cells were transiently transfected with either F-M2R or F-M2R-0cK and then plated on polylysine-coated glass coverslips. In some experiments, cells were co-transfected with, Rab7 or Rab11, GFP-HRS or GFP-TfnR. Cells were fed M1-563 anti-FLAG antibody for 30 minutes at 37°C before being treated with agonist for the indicated times and fixation with 4% formaldehyde in PBS. Fixation was quenched with TBS for 10 minutes before mounting or further processing. To label intracellular compartments, cells were permeablised and blocked (TBS, 0.1% Triton-X100, 3% BSA) for 30 minutes before incubation with antibody against EEA1 (1/200), or Rab11 (1/200) overnight at 4°C. Finally, cells were incubated with AF-488 labelled secondary (1/2000) for 1 hour at room temperature, before mounting on microscope slides for analysis by confocal fluorescence microscopy using a Zeiss LSM 710 microscope fitted with a Zeiss 63 x NA1.4 objective operated in single photon mode, with standard filter sets verified for lack of detectable cross-channel bleed through and standard (1 Airy disc) pinhole. Acquired optical sections were rendered using a 2 pixel median filter and the contrast enhanced equally across the whole image, before analysis with

ImageJ (Rasband, W.S., ImageJ, U. S. National Institutes of Health, Bethesda, Maryland, USA, https://imagej.nih.gov/ij/, 1997-2018). Colocalization was quantified by Manders' coefficient using thresholds using the JaCOP plugin (Bolte and Cordelieres, 2006). All experiments were repeated on 3-4 independent occasions, and colocalization determined on a cell by cell basis.

2.10 Measurement of recycling by Flow Cytometry

Recycling of Flag-tagged M2R or M2R-0cK was determined by flow cytometry as previously described (Thompson et al., 2014). Surface receptors were labelled with the calcium sensitive antibody anti-Flag M1 conjugated to AF647 (1:1,000) for 30 min, before stimulation with carbachol for 30 min. Following stimulation, cells were rapidly washed with PBS/EDTA (2 mM) to remove any surface antibody and either resuspended in PBS (containing Ca2+ and Mg2+) to measure endocytosis (as indicated by an increase in fluorescence due to internalization protecting from the PBS/EDTA wash) or returned to the incubator in the presence of PBS/EDTA to measure recycling (as determined by a loss of fluorescence over time). Following all treatments, cells were pelleted, washed, and resuspended in PBS (containing Ca^{2+} and Mg^{2+}). All time points were prepared in duplicate, and samples were analysed using a FACSCalibur (BD Biosciences) with 5,000 events being analysed in all cases.

2.11 Ratiometric analysis of internalization and recycling

Internalization and recycling of transfected DRG neurons was measured as previously described (Kotowski et al., 2011; Tanowitz and von Zastrow, 2003; Yu et al., 2010). Briefly, cells were plated onto poly-lysine coated coverslips and 48 hours later were incubated with anti-Flag M1 conjugated to AF-488 before agonist treatment. Cells were then fixed in freshly made 4% paraformaldehyde in PBS (100%). Parallel cells were then treated with agonist and then fixed (internal fraction) or washed in PBS/EDTA and the fixed (Strip control). A final set of cells were agonist treated, stripped and then returned to 37^{o}C for one hour before fixation (recycled fraction). All cells were then incubated under non-permeablising conditions with anti-mouse secondary labelled with AF594 as above. Neurons were analysed by fluorescent microscopy (Zeiss) with images being taken at both red and green emissions with a constant gain, and fluorescent intensities recorded and analysed using ImageJ, and the ratio of 594 to 488 fluorescence recorded. Internalisation was determined by the

following equation (1-(ratio 594:488 of internal fraction / ratio 594:488 of 100%) x 100. Recycling was determined by ((ratio 594:488 of recycled fraction - ratio 594:488 of strip) / (ratio 594:488 of 100% - ratio 594:488 of strip)) x 100. For each condition, 6-10 individual neurons were imaged and the 594:488 ratio determined. The mean ratios were then used to determine the internalised or recycled percentage for each n value

2.12 Statistical analysis

All analysis was carried out using GraphPad Prism software. All n values refer to individual, independent experiments unless otherwise stated. Unpaired t-test was used to compare colocalization data between treated and untreated conditions, and between receptor types. Two-Way ANOVA was used to determine significant effects over degradation and recycling time courses between receptor types.

3. Results

3.1 M2 Receptor undergoes lysosomal proteolysis in HEK 293 cells

We initially investigated the downregulation of the M2 receptor (M2R) using an N-terminally Flag-epitope-tagged human M2R (Hislop et al., 2009). We first identified the endocytic fate of the M2R by the use of confocal microscopy and markers of distinct endocytic compartments. M2R were transiently expressed in HEK 293 cells and incubated with fluorescently labelled M1 anti-flag antibody to label the surface receptor, before agonist treatment. In untreated cells, M2R staining is found exclusively at the plasma membrane with little observable constitutive internalization, or colocalization with any endocytic compartment (Supplemental Figure 1A-C). Following 30 minutes stimulation with 10 μM carbachol, M2R underwent translocation from the plasma membrane to discrete intracellular puncta. These puncta ranged in size from small vesicles to much larger endosomes (Fig.1A, arrow), with many found colocalized with the Early Endosome Antigen 1 (EEA1) marker (Fig.1D). After longer agonist treatment (120 and 180 minutes), M2R from the plasma membrane could be found colocalized with the late endosome marker Rab7 and also the lysosome marker LAMP1 (Fig.1B, C and D, Supplemental Fig.1F). These colocalization data suggest that the M2R might undergo rapid lysosomal proteolysis. To investigate this we used immunoblotting of the N-terminal Flag epitope as a measurement of proteolysis (Hislop et al., 2004). HEK 293 cells stably transfected with M2R were treated for increasing periods of time with 10 μM carbachol before lysis, separation by SDS-PAGE and detection by Western blotting using the anti-Flag antibody. In untreated cells, the M2R resolved as heterogeneous immunoreactive bands (Fig.1E), similar to other GPCRs (Hislop et al., 2011, 2004). The first of these (*) was a small band that resolved at the predicted weight of the M2R (~50kDa), a larger more prominent immunoreactive band was detected at ~60 kDa (#), and is likely the glycosylated monomeric surface expressed form of the M2R. Finally, a second highly prominent band was detected at >110 kDa, consistent with a dimeric form of M2R (‡, (Marsango et al., 2018)). Agonist treatment with 10 μM carbachol saw a rapid loss of immunoreactivity of the monomeric species after 1-hour treatment, and an increase of immunoreactivity at the higher molecular weight species, which in turn decreased following longer treatments (3 – 5 hours). Quantification of the whole lane revealed that there is a clear, agonist dependent loss of immunoreactivity with a t½ of 52 minutes (Fig.1F). Pre-treatment

of M2R expressing cells with either chloroquine or Ammonium Chloride (Fig.1G) which inhibit lysosomal function, significantly prevented the agonist-induced loss of immunoreactivity (Two-Way ANOVA: chloroquine ($F(3,24)=66.01$, $p<0.0001$; Ammonium Chloride $F(3,24)=23.63$, $p<0.0001$; Fig.1H), indicating that M2R undergoes agonist induced lysosomal proteolysis.

3.2 M2 Receptor proteolysis is regulated by ubiquitination and the ESCRT machinery.

Lysosomal trafficking for a large number of membrane proteins requires ubiquitination of lysine residues within the intracellular domain (Raiborg and Stenmark, 2009). Protein ubiquitination promotes interaction with a number of ubiquitin-interacting proteins, including those that comprise the ESCRT complex, that target the protein to the lysosome (Katzmann et al., 2002; Raiborg et al., 2003), however, the role of ubiquitination and the ESCRT has remained less clear for GPCRs (Hislop et al., 2009; Marchese and Trejo, 2013). To determine if ubiquitination and the ESCRT are responsible for regulating the lysosomal sorting of M2R, we initially investigated whether M2R colocalized with the core component of ESCRT 0, HRS (Bache et al., 2003). HEK 293 cells were transiently transfected with Flag-M2R and a low amount (100ng/9 cm^2 cells) of GFP-HRS. In untreated cells, M2R was observed at the plasma membrane (Fig. 2Ai), which redistributed to endosomal structures following agonist treatment (Fig. 2Aiv), which showed significant colocalization with HRS (Fig. 2iv-vi, Fig. 2B, $t(53)=11.71$, $p=2.27x10^{-16}$). This data indicates that HRS and the ESCRT might play a role in regulating the endocytic trafficking of the M2R. It was then investigated whether the colocalization with HRS was important for the proteolysis of M2R by the use of RNAi to reduce cellular levels of the HRS and the ESCRT I protein Tsg101 (Hislop et al., 2004). Following transfection with RNAi oligonucleotides, M2R expressing cells were treated with 10 μM carbachol before analysis by immunoblotting (Fig. 2C and D). As before, control transfected cells, showed rapid M2R proteolysis, which was significantly inhibited by the knockdown of either HRS or Tsg101 (Two-Way ANOVA: HRS - $F(3,32)=2.971$, $p=0.046$; Tsg101 - ($F(3,32)=3.709$, $p=0.021$), indicating that a functional ESCRT complex is critical for sorting of the M2R to the lysosome. Interestingly, transfection with RNAi against Tsg101 also reduced the levels of HRS expression, although not to the extent of that caused by HRS siRNA, as previously reported (Gullapalli et al., 2006). Although the mechanism that causes this

remains unknown, it is perhaps not surprising since Tsg101 and HRS form a complex (Lu et al., 2003).

The involvement of the ESCRT complex is suggestive of direct ubiquitination being a requirement for M2R trafficking and downregulation, however, this may not be the case since other GPCRs have been shown to require functional ESCRT without needing receptor ubiquitination for lysosomal trafficking (Hislop et al., 2004). This hypothesis was therefore investigated by determining whether the M2R underwent ubiquitination. HEK 293 cells expressing M2R were transiently transfected with HA tagged-ubiquitin (Hislop et al., 2009; Marchese et al., 2003) and treated with 10 μM carbachol, before lysis, immunoprecipitation and analysis by immunoblotting with anti-HA to detect ubiquitin. Very little signal was seen in HEK 293 cells not expressing receptors (Fig.3B, 293 lane), however, a distinctive immunoreactive smear was detected in M2R expressing cells, even in the absence of agonist (Fig.3C). A small signal was detected at the monomeric receptor (*), with greater immunoreactivity at higher molecular weights. The intensity of ubiquitination was mildly increased following receptor activation by carbachol, most noticeably at the monomeric species, (Fig.3B and D). Therefore, the M2R undergoes clear ubiquitination; however, this does not necessarily indicate a requirement for lysosomal trafficking (Hislop et al., 2004). To directly address this question we created a mutant M2R where all 28 intracellular lysine residues were mutated to arginine – M2R-0cK (Fig.3A), a strategy that has successfully been used to prevent ubiquitination of a number of GPCRs (Hislop et al., 2011; Marchese and Benovic, 2001; Shenoy et al., 2001; Tanowitz and Von Zastrow, 2002). Indeed, this receptor showed no basal ubiquitination and no increase in ubiquitination following agonist activation (Fig.3B, C and D). To further characterise the M2R-0cK, we first used immunofluorescent microscopy to follow its endosomal trafficking. Similarly, to the wild-type (WT) M2R, M2R-0cK was easily detected on the plasma membrane with little evidence of constitutive endocytosis (Supplemental Fig. 2A-C). Following agonist treatment, M2R-0cK was redistributed to endosomal compartments where colocalization was observed with EEA1, Rab7 and LAMP1 (Supplemental Fig.2A-C). Quantification of receptor endocytosis by flow cytometry revealed no difference between M2R and M2R-0cK (Supplemental Fig. D), indicating that the receptor can initiate endocytic trafficking identically to the WT receptor. Finally, we investigated whether the M2R-0cK is able to signal. Since endogenous

muscarinic receptors make signalling difficult to interpret, we made DREADD mutations (Armbruster et al., 2007) in both the WT and M2R-0cK. These two mutations confer on the receptor the ability to respond to clozapine-N-oxide (CNO), which does not activate other receptors. Western blotting of phospho-ERK levels following agonist stimulation revealed no difference between the M2R and the M2R-0cK in the response to CNO (Supplemental Fig. 2E). Together these data suggest that the lysine mutations have not altered the function of the M2R. Interestingly, upon quantification of M2R-0cK colocalization with endosomal markers, clear differences were observed between M2R and M2R-0cK (Supplemental Fig. 2F). Most strikingly, colocalization with both Rab7 and LAMP1 was significantly reduced for M2R-0cK compared to M2R (Rab7; $t(57)=15.16$, $p=1.08x10^{-21}$, DsRed-LAMP1; $t(50)=15.07$, $p=2.27x10^{-20}$), suggesting that ubiquitination might play a role in the lysosomal trafficking of M2R, and subsequent proteolysis.

To determine what role direct receptor ubiquitination had on M2R proteolysis, HEK 293 cells stably expressing M2R-0cK were stimulated with carbachol before lysis and immunoblotting. Similar to the WT, M2R-0cK resolved as heterogenous immunoreactive bands, however, in stark contrast to the wild-type M2R, M2R-0cK showed no change in receptor levels even after extended agonist treatments (Two-Way ANOVA: $F(3,48)=5.98$, $p=0.0015$, Fig. 3E and F). We then used the gold standard method of measuring mAChR downregulation, that of radioligand binding to [^{3}H]-Quinuclidinyl benzilate (QNB). As with the previous assays, cells stably expressing the wild-type M2R show a clear agonist-induced reduction in specific [^{3}H]-QNB binding, consistent with a loss of receptors. The t½ of 220 mins was slower than that seen for loss of epitope, consistent with the ligand binding site taking longer to be proteolyzed than the extracellular domain, but this rate was similar to that seen in other studies (Thangaraju and Sawyer, 2011). In contrast however, cells expressing M2R-0cK showed no decrease in [^{3}H]-QNB binding (Two-Way ANOVA: $F(3,30)=10.30$, $p<0.0001$, Fig.3G).

Finally, this critical result was verified by a biotin-protection-degradation assay to specifically follow the endocytic fate of the surface receptor (Thompson et al., 2014; Thompson and Whistler, 2011). The M2R underwent clear endocytosis (Fig.3H – 30 min) followed by a loss of signal after extended agonist treatments (Fig.3H and I), whereas the M2R-0cK underwent similar endocytosis but the endocytic pool was

maintained (Two-Way ANOVA: ($F(2,18)=19.29$, $p<0.0001$, Fig.3H and I). Together, these data show conclusively that ubiquitination of the M2R is required for agonist-induced lysosomal trafficking and downregulation.

3.3 Ubiquitin controls involution of the M2 Receptor

It is hypothesised that ubiquitination of receptors targets them for lysosomal proteolysis by promoting the transfer of receptors from the limiting membrane of the endosome to intraluminal vesicles (a process termed involution). This allows delivery of membrane cargo to the lumen of the lysosome following endosome fusion. To determine whether ubiquitination is regulating sorting of M2R, we first utilised a previously described involution assay (Supplemental Fig. 3 (Henry et al., 2011)). Both the M2R and M2R-0cK were C-terminally tagged in-frame with a pH-sensitive GFP variant – pHlorin. These receptors were then co-expressed with the mCherry-Rab5-Q79L constitutively active mutant to enlarge the endosomes to a point where the lumen can be clearly observed. In these cells, any receptors that are found in the lumen of the endosome are not fluorescent, due to the quenching nature of the low endosomal pH. The addition of chloroquine neutralises the luminal pH, revealing the presence of any tagged receptors within the lumen of the endosome (Fig.4A and B). Following agonist treatment for 90 mins, both the M2R and M2R-0cK can clearly be seen internalized from the plasma membrane onto the limiting membrane of the enlarged endosomal structures (Supplemental Fig.3B and C). Upon the addition of chloroquine, a large increase in intraluminal fluorescence was observed for the M2R (Fig.4A and C), consistent with a large proportion of receptor present within the lumen, whereas the M2R-0cK was largely excluded from the lumen (Fig.4B and C). These data indicate that ubiquitination of the M2R promotes sorting to the lysosome by increasing involution.

3.4 Ubiquitination of the M2 receptor controls post-endocytic sorting.

The above data clearly show that preventing ubiquitination prevents M2R involution and subsequent proteolysis (Fig.4 and 3). It has, however, previously been shown that involution does not necessarily determine whether a given GPCR undergoes

trafficking to the lysosome or is recycled to the plasma membrane (Henry et al., 2011; Hislop et al., 2011). If a receptor is prevented from trafficking to the lysosome, it might be predicted that the receptor may undergo recycling instead; however, for many GPCRs this is not the case (Thompson and Whistler, 2011). We used a previously described flow cytometry based assay to measure recycling of the endocytosed pool of receptors (Thompson et al., 2014). Agonist treatment of both M2R and M2R-0cK caused a similar, substantial increase in fluorescence compared to control cells, consistent with internalization of both receptors (Fig.5A and B, 30 min bar). Allowing the cells to recover for one hour in the absence of agonist showed only a small decrease in fluorescence of M2R expressing cells, indicating that the receptor was retained within the cell. This level of fluorescence was maintained for 3 hours after agonist removal, consistent with M2R not recycling and being trafficked to the late endosome. Similarly, after one hour's recovery, no reduction in fluorescence was seen in M2R-0cK expressing cells, however longer recovery periods (2 and 3 hours) showed a significant reduction in fluorescence (One-Way ANOVA: $F(15)=5.94$, $p=0.01$, Fig.5B) suggesting increased recycling of the M2R-0cK. Quantification of recycling of the internalized fraction revealed a significant increase of M2R-0cK when compared to M2R (Two-Way ANOVA: $F(2,18)=5.042$, $p=0.018$, Fig.5C), albeit slower than that typically seen for rapidly recycling receptors (Lauffer et al., 2010; Temkin et al., 2011).

We next used confocal microscopy to determine the route of M2R-0cK recycling. HEK 293 cells transiently expressing GFP-Rab11 and either M2R or M2R-0cK were fed M1 antibody. In cells not treated with agonist, both the M2R and M2R-0cK were found on the cell surface (Supplemental Fig. 4). Following addition of 10 μM carbachol for 90 minutes, both receptors underwent extensive internalization, however whereas the M2R was seen predominately in small vesicles, with a small number co-labelled with GFP-Rab11 (Fig.5D), M2R-0cK was seen to exhibit extensive colocalization with Rab11. Of particular note, the M2R-0cK was now found in a distinctive conglomerate of vesicles consistent with the perinuclear recycling compartment (Fig.5B, arrow). Quantification of colocalization showed a significant difference between M2R and M2R-0cK ($t(77)=7.133$, $p=4.66\times10^{-10}$, Fig. 5F), indicating a change in trafficking both qualitatively and quantifiably. These data show that ubiquitination of the M2R targets the receptor for lysosomal proteolysis and in its absence the receptor undergoes slow

recycling through the Rab11 recycling pathway (Innamorati et al., 2001; Ullrich et al., 1996; Wandinger-Ness and Zerial, 2014).

3.5 Ubiquitination regulates post-endocytic sorting in Dorsal root ganglia

The M2R has an important function in neurons where it is often found as a presynaptic auto-receptor or hetero-receptor (Lebois et al., 2018), and its downregulation has been implicated in a number of cognitive diseases (Dencker et al., 2012; Gibbons et al., 2016; Lebois et al., 2018). To determine if ubiquitin similarly regulates M2R trafficking in neurons, we used primary dissociated rat dorsal root ganglia neurons. These were transfected with either Flag tagged M2R or M2R-0cK and endocytic trafficking measured by ratiometric fluorescence assay (Supplemental Fig. 5 (Tanowitz and von Zastrow, 2003; Yu et al., 2010)). Under visual inspection, the M2R underwent endocytosis with many puncta seen in both the cell body and neurites, and the prevention of ubiquitination had no effect on this (Fig. 6A and B). Quantification revealed that both receptors underwent similar amount of internalization (Fig. 6C). In contrast, however, recycling was greatly increased by the prevention of ubiquitination. WT M2R underwent limited recycling (~30%) whereas M2R-0cK was recycled significantly more (~70%, $t(4)=2.652$, $p=0.0284$) after one hour following agonist washout (Fig. 6D). Finally, the M2R-0cK was again found to be colocalized with Rab11 (Fig. 6F), whereas only limited colocalization is seen with the WT M2R, consistent with the small amount of recycling observed (Fig. 6E). Together these data show that post-endocytic sorting of the M2 receptor is controlled by ubiquitination, a mechanism maintained in primary neurons.

4. Discussion

The Gi-coupled M2R plays important roles in the CNS where it is a critical presynaptic receptor that reduces neurotransmitter release, and can be found within the hypothalamus, hippocampus and neocortex (Lebois et al., 2018; Thomsen et al., 2018). The disruption of M2R signalling has important consequences within the CNS. M2R knockout mice show a number of cognitive deficits including working memory and spatial memory, and decreases in M2R levels have been shown in the cortex of

Alzheimer's patients as well as those with bipolar disorder (Gibbons et al., 2016; Kruse et al., 2014; Scarr, 2012; Thomsen et al., 2018). It is therefore critical for both understanding of the progression of these diseases and also the development of therapeutics to identify the molecular mechanisms regulating this process of M2R downregulation. Here we identify, for the first time, receptor ubiquitination as the critical regulator of M2R downregulation.

The model for ubiquitin dependent sorting to the lysosome has predominantly been based around early studies in yeast, where cargo destined for the vacuole undergoes ubiquitination of lysine residues which allows interaction with the ESCRT complex of ubiquitin interacting proteins (reviewed in (Haglund and Dikic, 2012; Katzmann et al., 2002; Raiborg and Stenmark, 2009; Saksena et al., 2007). The ESCRT complex has a dual role in both the binding and sorting of ubiquitinated cargo and also the formation of multivesicular bodies by the process of involution (Schoneberg et al., 2017). The combined function of the ESCRT both sorts and removes ubiquitinated cargo from the endosome membrane, translocating it into the endosome lumen, where it is accessible to lipases and proteases following fusion with the vacuole. The same process has been described for the lysosomal sorting of tyrosine kinase receptors in mammalian cells (Eden et al., 2009; Haglund and Dikic, 2012; Raiborg et al., 2003; Razi and Futter, 2006; Tomas et al., 2014), however, GPCR sorting appears to be more complicated process. Although it has been clear for many years that ubiquitin plays a central role in the downregulation of many GPCRs (Jacob et al., 2005; Marchese and Benovic, 2001; Martin et al., 2003; Shenoy et al., 2001), the specific action and requirement remains enigmatic and can vary between different receptors. Indeed, although clearly involved in the regulation of GPCR proteolysis, the actual role of ubiquitin in determining endocytic fate is far more complicated. For example, early studies into the downregulation of CXCR4 showed a clear requirement for both ubiquitination and the ESCRT complex and disruption of this process prevented sorting to the lysosomal compartment (Bhandari et al., 2009; Marchese et al., 2003; Marchese and Benovic, 2001). Similarly, PAR2 and NK1R also appear to be regulated by both direct ubiquitination and the ESCRT machinery, however, whether this is linked to involution remains unknown (Cottrell et al., 2006; Hasdemir et al., 2009, 2007; Jacob et al., 2005). In contrast, both the mu and delta opioid receptors (MOR and DOR respectively) undergo clear ubiquitination following agonist activation, however, this

process controls the involution into multivesicular bodies, and not the sorting to the lysosome (Henry et al., 2011; Hislop et al., 2011, 2009; Tanowitz and Von Zastrow, 2002), which appears to be governed by a ubiquitin-independent process, such as an interaction with GASP proteins (Thompson et al., 2007; Whistler et al., 2002). Finally, the PAR1 receptor is sorted to the lysosomes independently of both ubiquitination and the ESCRT components HRS and Tsg101 (Dores et al., 2016, 2012; Gullapalli et al., 2006). Despite the undoubted importance of how GPCRs undergo downregulation, the relevance of the ubiquitin-ESCRT model for this class of receptors remains under investigated.

Here we show that the M2R undergoes rapid sorting to the lysosome and this process is regulated by both ubiquitin and the ESCRT complex. Knockdown of both ESCRT 0 (HRS) and ESCRT I (Tsg101) reduced M2R proteolysis, and while it is possible that the observed effect of Tsg101 caused by a reduction of HRS (see Fig. 2D), we find this unlikely, since similar effect was not seen previously with the DOR, whose proteolysis is unaffected by Tsg101 RNAi (Hislop et al., 2004). Furthermore, we clearly identify that for the M2R, ubiquitination drives involution into multivesicular bodies, suggesting that involution is the primary mechanism by which M2R is sorted away from recycling pathways and towards the lysosome. Although consistent with the ubiquitin-ESCRT model described above, this would be the first demonstration of ubiquitin-dependent involution regulating sorting of a GPCR. Other GPCRs have been shown to require both ubiquitin and ESCRT machinery for lysosomal sorting (Hasdemir et al., 2007; Jacob et al., 2005; Marchese et al., 2003), however, the role of involution in the sorting of these receptors has largely been overlooked. Further, the time course of downregulation for those GPCRs regulated by ubiquitin is significantly slower than that shown for the M2R, raising the question of why there is such rapid involution and lysosomal sorting of the M2R? In addition to targeting receptors for degradation, rapid involution has also been proposed switch off signalling of tyrosine kinase receptors like the EGFR, by insulating it from cytosolic signalling cascades (Eden et al., 2009; Kostaras et al., 2013). It is interesting to speculate that a similar function may be occurring for the M2R. For GPCRs in general, there is renewed interest in signalling from the endosome, both through G-proteins and G-protein-independent pathways (Irannejad and von Zastrow, 2014; Peterson and Luttrell, 2017; Vilardaga et al., 2014). Although there is currently little evidence for

endosomal signalling of the M2R, it is interesting to note that M2R does form stable endosomal complexes with arrestin (Mosser et al., 2008), in which regard it is similar to both the Angiotensin II receptor and Vasopressin 2 receptor, both of which do exhibit extensive endosomal signalling (Jean-Charles et al., 2016; Peterson and Luttrell, 2017; Shenoy et al., 2009; Vilardaga et al., 2014). If such signalling is also observed for the M2R, then ubiquitin-ESCRT mediated involution would allow its rapid cessation, and offer a potential explanation for this rapid process, not seen in other GPCRs.

Interestingly, stable arrestin-receptor complexes, as seen for the M2R, have been suggested to be regulated by the ubiquitination state of arrestin, which controls both signalling and trafficking of the receptor (Berthouze et al., 2009; Shenoy and Lefkowitz, 2003). Indeed, the ubiquitination of arrestin has previously been shown to be a factor in controlling M2R downregulation (Mosser et al., 2008). The role of arrestin in downregulation, was not investigated in the current study, but it is worth noting that arrestins have been shown to interact with ESCRT and modulate the downregulation of the CXCR4 chemokine receptor, another GPCR which is predominantly sorted through ubiquitination (Bhandari et al., 2007; Malik et al., 2012).

One critical finding of this study is that the disruption of M2R ubiquitination not only prevented its lysosomal sorting, but also rerouted trafficking through Rab11 positive endosomes to be returned to the plasma membrane. These findings were somewhat surprising, since the lysosomal trafficking of rapidly degraded GPCRs (< 2hours) typically requires ubiquitin-independent processes (Whistler et al., 2002), and preventing ubiquitination does not therefore, cause a rerouting to the recycling pathway (Henry et al., 2011), although this has been partially observed for receptors that undergo lysosomal targeting with far slower kinetics (PAR2 and NK1, (Cottrell et al., 2006; Jacob et al., 2005)). This is an important distinction between M2R and previously described receptors such as the DOR and MOR, since it implies that the targeting of the ubiquitination process is a viable strategy for preventing downregulation and maintaining surface receptor number. The loss of functional receptors has, for some time, been a stumbling block for the use of agonists as therapeutics, as this can lead to pharmacological tolerance, reducing their clinical effectiveness. Further, the loss of functional muscarinic receptors is observed in a range of mental health disorders (Dencker et al., 2012; Lebois et al., 2018; Scarr, 2012). Combined, these data identify the downregulation of muscarinic acetylcholine

receptors as an important regulatory mechanism in disease states, and that preventing downregulation by targeting receptor ubiquitination has potential to reduce both tolerance and also reverse the symptoms of these disorders.

5. Acknowledgements

The authors would like to thank Professor Mark von Zastrow from the University of California, San Francisco for sharing critical constructs. We would like to thank Kevin MacKenzie and the University of Aberdeen Microscopy core and the Iain Fraser Flow cytometry core for their assistance in the acquisition of data, and Professor Lynda Erskine for critical reading of the manuscript.

This work was supported by a PhD studentship from the University of Aberdeen (DZ) and by funding from the Royal Society and Tenovus Scotland (JNH)

References

Armbruster, B.N., Li, X., Pausch, M.H., Herlitze, S., Roth, B.L., 2007. Evolving the lock to fit the key to create a family of G protein-coupled receptors potently activated by an inert ligand. Proc. Natl. Acad. Sci. U. S. A. 104, 5163–5168. https://doi.org/10.1073/pnas.0700293104

Bache, K.G., Brech, A., Mehlum, A., Stenmark, H., 2003. Hrs regulates multivesicular body formation via ESCRT recruitment to endosomes. J. Cell Biol. 162, 435–442. https://doi.org/10.1083/jcb.200302131

Bernard, V., Brana, C., Liste, I., Lockridge, O., Bloch, B., 2003. Dramatic depletion of cell surface m2 muscarinic receptor due to limited delivery from intracytoplasmic stores in neurons of acetylcholinesterase-deficient mice. Mol. Cell. Neurosci. 23, 121–133.

Bernard, V., Levey, A.I., Bloch, B., 1999. Regulation of the subcellular distribution of m4 muscarinic acetylcholine receptors in striatal neurons in vivo by the cholinergic environment: evidence for regulation of cell surface receptors by endogenous and exogenous stimulation. J. Neurosci. Off. J. Soc. Neurosci. 19, 10237–10249.

Berthouze, M., Venkataramanan, V., Li, Y., Shenoy, S.K., 2009. The deubiquitinases USP33 and USP20 coordinate beta2 adrenergic receptor recycling and resensitization. EMBO J. 28, 1684–1696. https://doi.org/10.1038/emboj.2009.128

Bhandari, D., Robia, S.L., Marchese, A., 2009. The E3 ubiquitin ligase atrophin interacting protein 4 binds directly to the chemokine receptor CXCR4 via a novel WW domain-mediated interaction. Mol. Biol. Cell 20, 1324–1339. https://doi.org/10.1091/mbc.e08-03-0308

Bhandari, D., Trejo, J., Benovic, J.L., Marchese, A., 2007. Arrestin-2 interacts with the ubiquitin-protein isopeptide ligase atrophin-interacting protein 4 and mediates endosomal sorting of the chemokine receptor CXCR4. J. Biol. Chem. 282, 36971–36979. https://doi.org/10.1074/jbc.M705085200

Bolte, S., Cordelieres, F.P., 2006. A guided tour into subcellular colocalization analysis in light microscopy. J. Microsc. 224, 213–232. https://doi.org/10.1111/j.1365-2818.2006.01706.x

Cottrell, G.S., Padilla, B., Pikios, S., Roosterman, D., Steinhoff, M., Gehringer, D., Grady, E.F., Bunnett, N.W., 2006. Ubiquitin-dependent down-regulation of the neurokinin-1 receptor. J. Biol. Chem. 281, 27773–27783. https://doi.org/10.1074/jbc.M603369200

Decossas, M., Doudnikoff, E., Bloch, B., Bernard, V., 2005. Aging and subcellular localization of m2 muscarinic autoreceptor in basalocortical neurons in vivo. Neurobiol. Aging 26, 1061–1072. https://doi.org/10.1016/j.neurobiolaging.2004.09.007

Dencker, D., Thomsen, M., Wortwein, G., Weikop, P., Cui, Y., Jeon, J., Wess, J., Fink-Jensen, A., 2012. Muscarinic Acetylcholine Receptor Subtypes as Potential Drug Targets for the Treatment of Schizophrenia, Drug Abuse and Parkinson's Disease. ACS Chem. Neurosci. 3, 80–89. https://doi.org/10.1021/cn200110q

Dores, M.R., Grimsey, N.J., Mendez, F., Trejo, J., 2016. ALIX Regulates the Ubiquitin-Independent Lysosomal Sorting of the P2Y1 Purinergic Receptor via a YPX3L Motif. PloS One 11, e0157587. https://doi.org/10.1371/journal.pone.0157587

Dores, M.R., Paing, M.M., Lin, H., Montagne, W.A., Marchese, A., Trejo, J., 2012. AP-3 regulates PAR1 ubiquitin-independent MVB/lysosomal sorting via an. Mol. Biol. Cell 23, 3612–3623. https://doi.org/10.1091/mbc.E12-03-0251

Eden, E.R., Huang, F., Sorkin, A., Futter, C.E., 2012. The role of EGF receptor ubiquitination in regulating its intracellular traffic. Traffic Cph. Den. 13, 329–337. https://doi.org/10.1111/j.1600-0854.2011.01305.x

Eden, E.R., White, I.J., Futter, C.E., 2009. Down-regulation of epidermal growth factor receptor signalling within multivesicular bodies. Biochem. Soc. Trans. 37, 173–177. https://doi.org/10.1042/BST0370173

Felder, C.C., Bymaster, F.P., Ward, J., DeLapp, N., 2000. Therapeutic opportunities for muscarinic receptors in the central nervous system. J. Med. Chem. 43, 4333–4353.

Ferguson, S.S., 2001. Evolving concepts in G protein-coupled receptor endocytosis: the role in receptor desensitization and signaling. Pharmacol. Rev. 53, 1–24.

Gibbons, A.S., Jeon, W.J., Scarr, E., Dean, B., 2016. Changes in Muscarinic M2 Receptor Levels in the Cortex of Subjects with Bipolar Disorder and Major Depressive Disorder and in Rats after Treatment with Mood Stabilisers and Antidepressants. Int. J. Neuropsychopharmacol. 19. https://doi.org/10.1093/ijnp/pyv118

Gibbons, A.S., Scarr, E., Boer, S., Money, T., Jeon, W.-J., Felder, C., Dean, B., 2013. Widespread decreases in cortical muscarinic receptors in a subset of people with schizophrenia. Int. J. Neuropsychopharmacol. 16, 37–46. https://doi.org/10.1017/S1461145712000028

Gullapalli, A., Wolfe, B.L., Griffin, C.T., Magnuson, T., Trejo, J., 2006. An essential role for SNX1 in lysosomal sorting of protease-activated receptor-1: evidence for retromer-, Hrs-, and Tsg101-independent functions of sorting nexins. Mol. Biol. Cell 17, 1228–1238. https://doi.org/10.1091/mbc.e05-09-0899

Gurevich, V.V., Dion, S.B., Onorato, J.J., Ptasienski, J., Kim, C.M., Sterne-Marr, R., Hosey, M.M., Benovic, J.L., 1995. Arrestin interactions with G protein-coupled receptors. Direct binding studies of wild type and mutant arrestins with rhodopsin, beta 2-adrenergic, and m2 muscarinic cholinergic receptors. J. Biol. Chem. 270, 720–731. https://doi.org/10.1074/jbc.270.2.720

Haglund, K., Dikic, I., 2012. The role of ubiquitylation in receptor endocytosis and endosomal sorting. J. Cell Sci. 125, 265–275. https://doi.org/10.1242/jcs.091280

Hanyaloglu, A.C., von Zastrow, M., 2008. Regulation of GPCRs by endocytic membrane trafficking and its potential implications. Annu. Rev. Pharmacol. Toxicol. 48, 537–568. https://doi.org/10.1146/annurev.pharmtox.48.113006.094830

Hasdemir, B., Bunnett, N.W., Cottrell, G.S., 2007. Hepatocyte growth factor-regulated tyrosine kinase substrate (HRS) mediates post-endocytic trafficking of protease-activated receptor 2 and calcitonin receptor-like receptor. J. Biol. Chem. 282, 29646–29657. https://doi.org/10.1074/jbc.M702974200

Hasdemir, B., Murphy, J.E., Cottrell, G.S., Bunnett, N.W., 2009. Endosomal deubiquitinating enzymes control ubiquitination and down-regulation of protease-activated receptor 2. J. Biol. Chem. 284, 28453–28466. https://doi.org/10.1074/jbc.M109.025692

Henry, A.G., White, I.J., Marsh, M., von Zastrow, M., Hislop, J.N., 2011. The role of ubiquitination in lysosomal trafficking of delta-opioid receptors. Traffic Cph. Den. 12, 170–184. https://doi.org/10.1111/j.1600-0854.2010.01145.x

Hicke, L., Riezman, H., 1996. Ubiquitination of a yeast plasma membrane receptor signals its ligand-stimulated endocytosis. Cell 84, 277–287. https://doi.org/10.1016/s0092-8674(00)80982-4

Hislop, J.N., Henry, A.G., Marchese, A., von Zastrow, M., 2009. Ubiquitination regulates proteolytic processing of G protein-coupled receptors after their sorting to lysosomes. J. Biol. Chem. 284, 19361–19370. https://doi.org/10.1074/jbc.M109.001644

Hislop, J.N., Henry, A.G., von Zastrow, M., 2011. Ubiquitination in the first cytoplasmic loop of mu-opioid receptors reveals a hierarchical mechanism of lysosomal down-regulation. J. Biol. Chem. 286, 40193–40204. https://doi.org/10.1074/jbc.M111.288555

Hislop, J.N., Marley, A., Von Zastrow, M., 2004. Role of mammalian vacuolar protein-sorting proteins in endocytic trafficking of a non-ubiquitinated G protein-coupled receptor to lysosomes. J. Biol. Chem. 279, 22522–22531. https://doi.org/10.1074/jbc.M311062200

Hislop, J.N., von Zastrow, M., 2011. Role of ubiquitination in endocytic trafficking of G-protein-coupled receptors. Traffic Cph. Den. 12, 137–148. https://doi.org/10.1111/j.1600-0854.2010.01121.x

Hosey, M.M., Pals-Rylaarsdam, R., Lee, K.B., Roseberry, A.G., Benovic, J.L., Gurevich, V.V., Bunemann, M., 1999. Molecular events associated with the regulation of signaling by M2 muscarinic receptors. Life Sci. 64, 363–368. https://doi.org/10.1016/s0024-3205(98)00575-x

Innamorati, G., Le Gouill, C., Balamotis, M., Birnbaumer, M., 2001. The long and the short cycle. Alternative intracellular routes for trafficking of. J. Biol. Chem. 276, 13096–13103. https://doi.org/10.1074/jbc.M009780200

Irannejad, R., von Zastrow, M., 2014. GPCR signaling along the endocytic pathway. Curr. Opin. Cell Biol. 27, 109–116. https://doi.org/10.1016/j.ceb.2013.10.003

Jacob, C., Cottrell, G.S., Gehringer, D., Schmidlin, F., Grady, E.F., Bunnett, N.W., 2005. c-Cbl mediates ubiquitination, degradation, and down-regulation of human protease-activated receptor 2. J. Biol. Chem. 280, 16076–16087. https://doi.org/10.1074/jbc.M500109200

Jean-Charles, P.-Y., Rajiv, V., Shenoy, S.K., 2016. Ubiquitin-Related Roles of beta-Arrestins in Endocytic Trafficking and Signal Transduction. J. Cell. Physiol. 231, 2071–2080. https://doi.org/10.1002/jcp.25317

Katzmann, D.J., Odorizzi, G., Emr, S.D., 2002. Receptor downregulation and multivesicular-body sorting. Nat. Rev. Mol. Cell Biol. 3, 893–905. https://doi.org/10.1038/nrm973

Kostaras, E., Sflomos, G., Pedersen, N.M., Stenmark, H., Fotsis, T., Murphy, C., 2013. SARA and RNF11 interact with each other and ESCRT-0 core proteins and regulate degradative EGFR trafficking. Oncogene 32, 5220–5232. https://doi.org/10.1038/onc.2012.554

Kotowski, S.J., Hopf, F.W., Seif, T., Bonci, A., von Zastrow, M., 2011. Endocytosis promotes rapid dopaminergic signaling. United States.

Krupnick, J.G., Benovic, J.L., 1998. The role of receptor kinases and arrestins in G protein-coupled receptor regulation. Annu. Rev. Pharmacol. Toxicol. 38, 289–319. https://doi.org/10.1146/annurev.pharmtox.38.1.289

Kruse, A.C., Kobilka, B.K., Gautam, D., Sexton, P.M., Christopoulos, A., Wess, J., 2014. Muscarinic acetylcholine receptors: novel opportunities for drug development. Nat. Rev. Drug Discov. 13, 549–560. https://doi.org/10.1038/nrd4295

Langmead, C.J., Watson, J., Reavill, C., 2008. Muscarinic acetylcholine receptors as CNS drug targets. Pharmacol. Ther. 117, 232–243. https://doi.org/10.1016/j.pharmthera.2007.09.009

Lauffer, B.E.L., Melero, C., Temkin, P., Lei, C., Hong, W., Kortemme, T., von Zastrow, M., 2010. SNX27 mediates PDZ-directed sorting from endosomes to the plasma membrane. J. Cell Biol. 190, 565–574. https://doi.org/10.1083/jcb.201004060

Lebois, E.P., Thorn, C., Edgerton, J.R., Popiolek, M., Xi, S., 2018. Muscarinic receptor subtype distribution in the central nervous system and relevance to aging and Alzheimer's disease. Neuropharmacology 136, 362–373. https://doi.org/10.1016/j.neuropharm.2017.11.018

Levey, A.I., 1996. Muscarinic acetylcholine receptor expression in memory circuits: implications for treatment of Alzheimer disease. Proc. Natl. Acad. Sci. U. S. A. 93, 13541–13546.

Lu, Q., Hope, L.W., Brasch, M., Reinhard, C., Cohen, S.N., 2003. TSG101 interaction with HRS mediates endosomal trafficking and receptor down-regulation. Proc. Natl. Acad. Sci. U. S. A. 100, 7626–7631. https://doi.org/10.1073/pnas.0932599100

Malik, R., Soh, U.J.K., Trejo, J., Marchese, A., 2012. Novel roles for the E3 ubiquitin ligase atrophin-interacting protein 4 and signal transduction adaptor molecule 1 in G protein-coupled receptor signaling. J. Biol. Chem. 287, 9013–9027. https://doi.org/10.1074/jbc.M111.336792

Marchese, A., Benovic, J.L., 2001. Agonist-promoted ubiquitination of the G protein-coupled receptor CXCR4 mediates lysosomal sorting. J. Biol. Chem. 276, 45509–45512. https://doi.org/10.1074/jbc.C100527200

Marchese, A., Raiborg, C., Santini, F., Keen, J.H., Stenmark, H., Benovic, J.L., 2003. The E3 ubiquitin ligase AIP4 mediates ubiquitination and sorting of the G protein-coupled receptor CXCR4. Dev. Cell 5, 709–722.

Marchese, A., Trejo, J., 2013. Ubiquitin-dependent regulation of G protein-coupled receptor trafficking and signaling. Cell. Signal. 25, 707–716. https://doi.org/10.1016/j.cellsig.2012.11.024

Marsango, S., Ward, R.J., Alvarez-Curto, E., Milligan, G., 2018. Muscarinic receptor oligomerization. Neuropharmacology 136, 401–410. https://doi.org/10.1016/j.neuropharm.2017.11.023

Martin, N.P., Lefkowitz, R.J., Shenoy, S.K., 2003. Regulation of V2 vasopressin receptor degradation by agonist-promoted ubiquitination. J. Biol. Chem. 278, 45954–45959. https://doi.org/10.1074/jbc.M308285200

McKinzie, D.L., Bymaster, F.P., 2012. Muscarinic mechanisms in psychotic disorders. Handb. Exp. Pharmacol. 233–265. https://doi.org/10.1007/978-3-642-25758-2_9

Mosser, V.A., Jones, K.T., Hoffman, K.M., McCarty, N.A., Jackson, D.A., 2008. Differential role of beta-arrestin ubiquitination in agonist-promoted down-regulation of M1 vs M2 muscarinic acetylcholine receptors. J. Mol. Signal. 3, 20. https://doi.org/10.1186/1750-2187-3-20

Pals-Rylaarsdam, R., Gurevich, V.V., Lee, K.B., Ptasienski, J.A., Benovic, J.L., Hosey, M.M., 1997. Internalization of the m2 muscarinic acetylcholine receptor. Arrestin-independent and -dependent pathways. J. Biol. Chem. 272, 23682–23689. https://doi.org/10.1074/jbc.272.38.23682

Peterson, Y.K., Luttrell, L.M., 2017. The Diverse Roles of Arrestin Scaffolds in G Protein-Coupled Receptor Signaling. Pharmacol. Rev. 69, 256–297. https://doi.org/10.1124/pr.116.013367

Pierce, K.L., Luttrell, L.M., Lefkowitz, R.J., 2001. New mechanisms in heptahelical receptor signaling to mitogen activated protein kinase cascades. Oncogene 20, 1532–1539. https://doi.org/10.1038/sj.onc.1204184

Raiborg, C., Rusten, T.E., Stenmark, H., 2003. Protein sorting into multivesicular endosomes. Curr. Opin. Cell Biol. 15, 446–455. https://doi.org/10.1016/s0955-0674(03)00080-2

Raiborg, C., Stenmark, H., 2009. The ESCRT machinery in endosomal sorting of ubiquitylated membrane proteins. Nature 458, 445–452. https://doi.org/10.1038/nature07961

Razi, M., Futter, C.E., 2006. Distinct roles for Tsg101 and Hrs in multivesicular body formation and inward vesiculation. Mol. Biol. Cell 17, 3469–3483. https://doi.org/10.1091/mbc.e05-11-1054

Reiner, C., Nathanson, N.M., 2012. Muscarinic receptor trafficking. Handb. Exp. Pharmacol. 61–78. https://doi.org/10.1007/978-3-642-23274-9_4

Saksena, S., Sun, J., Chu, T., Emr, S.D., 2007. ESCRTing proteins in the endocytic pathway. Trends Biochem. Sci. 32, 561–573. https://doi.org/10.1016/j.tibs.2007.09.010

Scarr, E., 2012. Muscarinic receptors: their roles in disorders of the central nervous system and potential as therapeutic targets. CNS Neurosci. Ther. 18, 369–379. https://doi.org/10.1111/j.1755-5949.2011.00249.x

Scarr, E., Udawela, M., Thomas, E.A., Dean, B., 2018. Changed gene expression in subjects with schizophrenia and low cortical muscarinic M1 receptors predicts disrupted upstream pathways interacting with that receptor. Mol. Psychiatry 23, 295–303. https://doi.org/10.1038/mp.2016.195

Schlador, M.L., Nathanson, N.M., 1997. Synergistic regulation of m2 muscarinic acetylcholine receptor desensitization and sequestration by G protein-coupled receptor kinase-2 and beta-arrestin-1. J. Biol. Chem. 272, 18882–18890. https://doi.org/10.1074/jbc.272.30.18882

Schoneberg, J., Lee, I.-H., Iwasa, J.H., Hurley, J.H., 2017. Reverse-topology membrane scission by the ESCRT proteins. Nat. Rev. Mol. Cell Biol. 18, 5–17. https://doi.org/10.1038/nrm.2016.121

Shenoy, S.K., Lefkowitz, R.J., 2003. Trafficking patterns of beta-arrestin and G protein-coupled receptors determined by the kinetics of beta-arrestin deubiquitination. J. Biol. Chem. 278, 14498–14506. https://doi.org/10.1074/jbc.M209626200

Shenoy, S.K., McDonald, P.H., Kohout, T.A., Lefkowitz, R.J., 2001. Regulation of receptor fate by ubiquitination of activated beta 2-adrenergic receptor and beta-arrestin. Science 294, 1307–1313. https://doi.org/10.1126/science.1063866

Shenoy, S.K., Modi, A.S., Shukla, A.K., Xiao, K., Berthouze, M., Ahn, S., Wilkinson, K.D., Miller, W.E., Lefkowitz, R.J., 2009. Beta-arrestin-dependent signaling and trafficking of 7-transmembrane receptors is reciprocally regulated by the deubiquitinase USP33 and the E3 ligase Mdm2. Proc. Natl. Acad. Sci. U. S. A. 106, 6650–6655. https://doi.org/10.1073/pnas.0901083106

Sherer, N.M., Lehmann, M.J., Jimenez-Soto, L.F., Ingmundson, A., Horner, S.M., Cicchetti, G., Allen, P.G., Pypaert, M., Cunningham, J.M., Mothes, W., 2003. Visualization of retroviral replication in living cells reveals budding into multivesicular bodies. Traffic Cph. Den. 4, 785–801.

Skieterska, K., Rondou, P., Van Craenenbroeck, K., 2017. Regulation of G Protein-Coupled Receptors by Ubiquitination. Int. J. Mol. Sci. 18. https://doi.org/10.3390/ijms18050923

Sorkin, A., Von Zastrow, M., 2002. Signal transduction and endocytosis: close encounters of many kinds. Nat. Rev. Mol. Cell Biol. 3, 600–614. https://doi.org/10.1038/nrm883

Tanowitz, M., von Zastrow, M., 2003. A novel endocytic recycling signal that distinguishes the membrane trafficking of naturally occurring opioid receptors. J. Biol. Chem. 278, 45978–45986. https://doi.org/10.1074/jbc.M304504200

Tanowitz, M., Von Zastrow, M., 2002. Ubiquitination-independent trafficking of G protein-coupled receptors to lysosomes. J. Biol. Chem. 277, 50219–50222. https://doi.org/10.1074/jbc.C200536200

Temkin, P., Lauffer, B., Jager, S., Cimermancic, P., Krogan, N.J., von Zastrow, M., 2011. SNX27 mediates retromer tubule entry and endosome-to-plasma membrane trafficking of signalling receptors. Nat. Cell Biol. 13, 715–721. https://doi.org/10.1038/ncb2252

Thangaraju, A., Sawyer, G.W., 2011. Comparison of the kinetics and extent of muscarinic M1-M5 receptor internalization, recycling and downregulation in Chinese hamster ovary cells. Eur. J. Pharmacol. 650, 534–543. https://doi.org/10.1016/j.ejphar.2010.10.054

Thompson, D., McArthur, S., Hislop, J.N., Flower, R.J., Perretti, M., 2014. Identification of a novel recycling sequence in the C-tail of FPR2/ALX receptor: association with cell protection from apoptosis. J. Biol. Chem. 289, 36166–36178. https://doi.org/10.1074/jbc.M114.612630

Thompson, D., Pusch, M., Whistler, J.L., 2007. Changes in G protein-coupled receptor sorting protein affinity regulate postendocytic targeting of G protein-coupled receptors. J. Biol. Chem. 282, 29178–29185. https://doi.org/10.1074/jbc.M704014200

Thompson, D., Whistler, J.L., 2011. Dopamine D(3) receptors are down-regulated following heterologous endocytosis by a specific interaction with G protein-coupled receptor-associated sorting protein-1. J. Biol. Chem. 286, 1598–1608. https://doi.org/10.1074/jbc.M110.158345

Thomsen, M., Sorensen, G., Dencker, D., 2018. Physiological roles of CNS muscarinic receptors gained from knockout mice. Neuropharmacology 136, 411–420. https://doi.org/10.1016/j.neuropharm.2017.09.011

Tomas, A., Futter, C.E., Eden, E.R., 2014. EGF receptor trafficking: consequences for signaling and cancer. Trends Cell Biol. 24, 26–34. https://doi.org/10.1016/j.tcb.2013.11.002

Ullrich, O., Reinsch, S., Urbe, S., Zerial, M., Parton, R.G., 1996. Rab11 regulates recycling through the pericentriolar recycling endosome. J. Cell Biol. 135, 913–924.

van Koppen, C.J., 2001. Multiple pathways for the dynamin-regulated internalization of muscarinic acetylcholine receptors. Biochem. Soc. Trans. 29, 505–508.

Vilardaga, J.-P., Jean-Alphonse, F.G., Gardella, T.J., 2014. Endosomal generation of cAMP in GPCR signaling. Nat. Chem. Biol. 10, 700–706. https://doi.org/10.1038/nchembio.1611

Wandinger-Ness, A., Zerial, M., 2014. Rab proteins and the compartmentalization of the endosomal system. Cold Spring Harb. Perspect. Biol. 6, a022616. https://doi.org/10.1101/cshperspect.a022616

Wess, J., Eglen, R.M., Gautam, D., 2007. Muscarinic acetylcholine receptors: mutant mice provide new insights for drug development. Nat. Rev. Drug Discov. 6, 721–733. https://doi.org/10.1038/nrd2379

Whistler, J.L., Enquist, J., Marley, A., Fong, J., Gladher, F., Tsuruda, P., Murray, S.R., Von Zastrow, M., 2002. Modulation of postendocytic sorting of G protein-coupled receptors. Science 297, 615–620. https://doi.org/10.1126/science.1073308

Yu, Y.J., Dhavan, R., Chevalier, M.W., Yudowski, G.A., von Zastrow, M., 2010. Rapid delivery of internalized signaling receptors to the somatodendritic surface by sequence-specific local

insertion. J. Neurosci. Off. J. Soc. Neurosci. 30, 11703–11714. https://doi.org/10.1523/JNEUROSCI.6282-09.2010

Zenko, D., Hislop, J.N., 2018. Regulation and trafficking of muscarinic acetylcholine receptors. Neuropharmacology 136, 374–382. https://doi.org/10.1016/j.neuropharm.2017.11.017

Figure Legends

Figure 1 – M2R undergoes lysosomal proteolysis

A-C) HEK 293 cells were transiently transfected with N terminally Flag-tagged M2R (F-M2R) and the indicated marker and plated on coverslips. Cells were fed with AF-M1 antibody (magenta) and treated with carbachol (10 μM) as indicated, before fixing and staining. A) M2R-AF568 (magenta, i) and cells stained with anti-EEA1 (green, ii). B) M2R-AF-568 (magenta, i) and GFP-Rab7 (green, ii). C) M2R-AF488 (magenta, i) and DsRed-LAMP1 (green, ii). Dotted lines show the outline of the cells, arrows show areas of colocalization (white). D) Quantification of colocalization using Manders' coefficient. Graph shows colocalization with the indicated marker following agonist treatment for the indicated time (EEA1, n=50 cells; GFP-Rab7, n=40 cells; LAMP1, n=38 cells, images taken from 3-4 independent experiments). E-F) HEK 293 stably expressing F-M2R were treated for the indicated time with 10μM carbachol, before lysis and SDS-PAGE. Shown is a representative anti-Flag Western blot, with quantification by densitometry (mean ± SEM, n=7, t½ determined by non-linear regression assuming a single exponential). G-H) F-M2R cells were pre-treated for 30 mins with chloroquine or Ammonium Chloride before treated for the indicated time with 10μM carbachol and Western blotting. Shown are representative anti-Flag Western blots, quantified by densitometry (mean ± SEM, n=4. Two-Way ANOVA: chloroquine; $F(3,24)=66.01$, $p<0.0001$; Ammonium Chloride; $F(3,24)=23.63$, $p<0.0001$, post-test statistics shown on graph, H).

Figure 2 – ESCRT is required for M2R proteolysis

A-B) HEK 293 cells were transiently transfected with F-M2R (1μg) and GFP-HRS (100ng) and plated on coverslips. Cells were fed with AF-568-M1 antibody (magenta, i and iv) for 30 mins before left untreated or treated with carbachol (10μM) for 30 mins, followed by fixation in 4% formaldehyde, and analysed by confocal microscopy. B shows quantification of colocalization using Manders' coefficient (unpaired t-test: $t(53)=11.71$, $p=2.27\times10^{-16}$. C-D) HEK 293 stably expressing F-M2R were transfected with the indicated siRNA, replated and 72 hours later treated for the indicated time with 10μM carbachol, before lysis and SDS-PAGE. Shown is a representative anti-Flag Western blot (D), with quantification by densitometry (mean ± SEM, n=5. Two-Way ANOVA: HRS; $F(3,32)=2.971$, $p=0.046$, TSG101; $F(3,32)=3.709$, $p=0.021$,

Bonferroni post hoc test shown on graph, D). Blots were stripped and reprobed with anti-HRS or anti-Tsg101.

Figure 3 – Ubiquitination is required for M2R proteolysis

A) Schematic representation of the M2R indicating the position of the 28 lysine residues replaced with arginine. B-D) HEK 293 calls stably transfected with F-M2R or F-M2R-0cK, were transiently transfected with HA-Ubiquitin, before treatment with 10μM carbachol for the indicated time, and lysis (see method) and SDS-PAGE. Shown is a representative anti-HA Western blot. These were quantified (mean ± SEM, n=4), to show the level of ubiquitination in unstimulated cells compared to receptor null cells (C, One-Way ANOVA: $F(3)=9.299$, $p=0.065$, C), and the agonist induced ubiquitination effect compared to untransfected cells (D mean ± SEM, n=4, Two-Way ANOVA: $F(4,30)=0.23$, $p=0.917$). E-F) M2R or M2R-0cK cells were treated with 10μM carbachol for the indicated time before lysis and Western blotting. Shown is a representative anti-Flag Western blot (E), and quantification by densitometry (mean ± SEM, n=7. Two-Way ANOVA: $F(3,48)=5.978$, $p=0.0015$, Bonferroni post hoc test shown on graph F). G) M2R or M2R-0cK cells were treated with 10μM carbachol for the indicated time before washing and freeze-thaw in PBS followed by radioligand binding with [^{3}H]-QNB (mean ± SEM, n=6. Two-Way ANOVA: $F(3,30)=10.3$, $p<0.0001$. Bonferroni post hoc test shown on graph, G). H-I) Biotin-Protection assay of M2R and M2R-0cK to show the fate of surface receptors. Shown is a representative blot probed with streptavidin-HRP to label biotinylated proteins (H). 100% lane is total surface receptor, strip represents efficiency of strip, non-treated is cells incubated in the absence of agonist. Blots were quantified by densitometry (mean ± SEM, n=4. Two-Way ANOVA: $F(2,18)=19.29$, $p<0.0001$, Bonferroni post hoc test values shown)

Figure 4 – Ubiquitination regulates the involution of the M2R.

HEK 293 cells were transiently transfected with mCherry-Rab5-Q79L and ether F-M2R-SEP (A) or F-M2R-0cK-SEP (B) and plated on coverslips. Cells were then treated with carbachol (10μM) for 90 mins and imaged by spinning disc confocal microscopy. Cells were imaged for 1 minute, before chloroquine (500 μM) was added. Shown is a representative image series of a single enlarged endosomes (scale bar = 5 μM, showing the increase in intraluminal fluorescence, following neutralization of the endosome lumen. Data is illustrative of four independent days of experimentation. The

increase in luminal fluorescence was then quantified (M2R, n=12 cells, 50 endosomes and M2R-0cK, n=14 cells, 47 endosomes, unpaired t-test; $t(84)=9.07$, $p=4.3x10^{-14}$).

Figure 5 – Ubiquitination regulates endocytic sorting of the M2R.

HEK 293 cells were transiently transfected with F-M2R (A) or F-M2R-0cK (B), and analysed by FACS for recycling. Cells were incubated with anti-Flag-AF647 before agonist treatment with carbachol for 30 min. Cells were washed with PBS-EDTA to remove remaining surface staining and then incubated at 37^{o}C for 60, 120 or 180 minutes, and remaining fluorescence measured (mean ± SEM, n=4. One-Way ANOVA: M2R - $F(15)=1.829$, $p=0.196$; M2R-0cK – $F(15)=5.94$, $p=0.01$, post-hoc tests shown on graph B). The extent of recycling (C) was determined by the amount of fluorescence caused by internalization remaining following the recovery period (mean ± SEM, n=4. Two-Way ANOVA: $F(2,18)=5.042$, $p=0.018$, with post-hoc test values shown). D and E) HEK 293 cells were transiently transfected with F-M2R (D) or F-M2R-0cK (E) and GFP-Rab11 (ii) and plated on coverslips. Cells were fed with AF-568-M1 antibody (magenta, i) and treated with carbachol (10 μM) for 90 mins, before fixing. Dotted lines show the outline of the cell and arrows indicate the Rab11 +ve recycling compartment. F) Colocalization was quantified using Manders' coefficient (M2R, 39 cells, M2R-0cK, 40 cells, unpaired t-test: $t(77)=7.133$, $p=4.66x10^{-10}$).

Figure 6 – Ubiquitination regulates the endocytic sorting of M2R in primary cultured DRGs.

DRG cultures transfected with F-M2R (A) or F-M2R-0cK (B) were fed with anti-FLAG-M1-AF-488 (green) before agonist treatment (Aii and Bii) and fixation under non-permeabilizing conditions. Cells were then stained with anti-mouse-AF-594, to label any antibody still on the cell surface surface (magenta), scale bars represent 10 μM. Ratiometric analysis was then used to determine internalisation (C) and Recycling (D) (Yu et al., 2010), (mean ± SEM, n=3, unpaired t-test t: Internalization – $t(4)=0.073$, Recycling – $t(4)=2.652$). E and F) DRG cells were fed M1-568, treated with carbachol for 90 minutes, before fixing and staining with anti-Rab11 antibody. Images show representative cell bodies, and dotted line shows area of neurite expanded in the lower images.

Figure 1

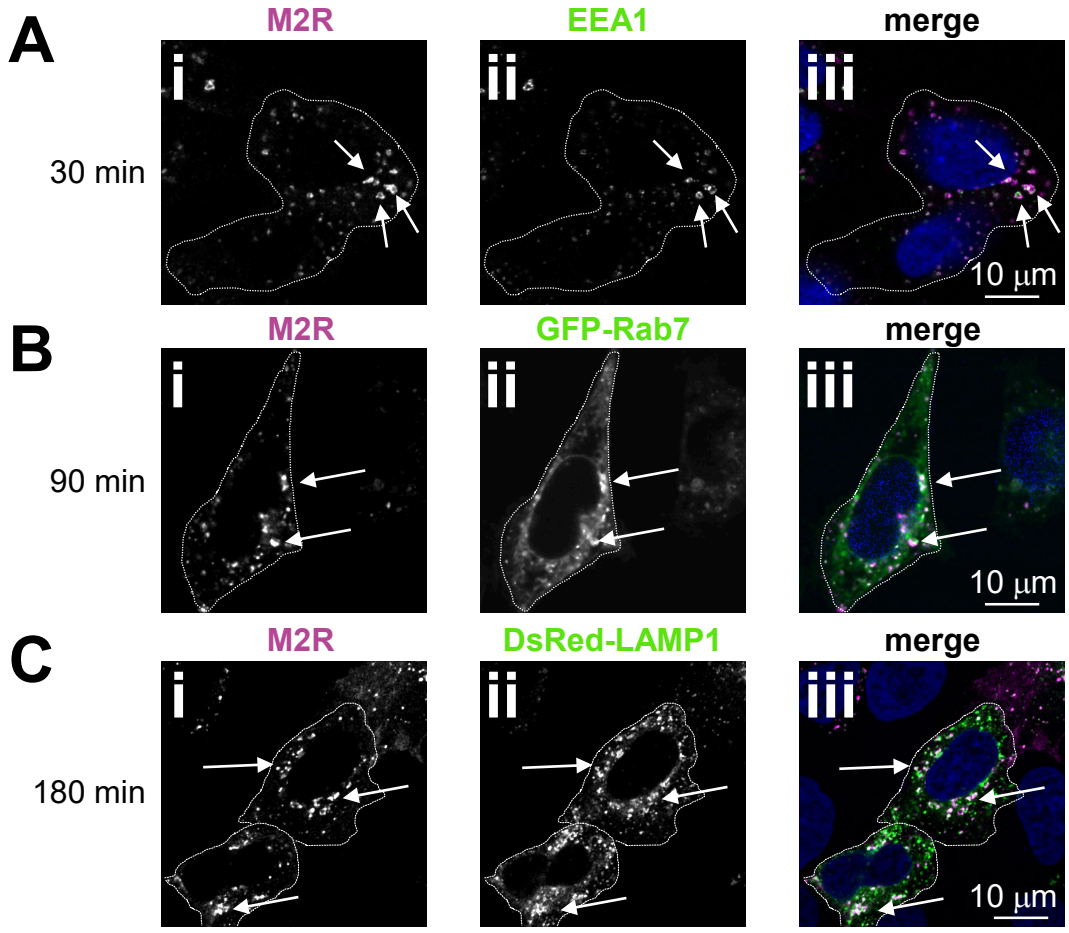
A
M2R
EEA1
merge
i
ii
iii
30 min
10 µm
B
M2R
GFP-Rab7
merge
i
ii
iii
90 min
10 µm
C
M2R
DsRed-LAMP1
merge
i
ii
iii
180 min
10 µm

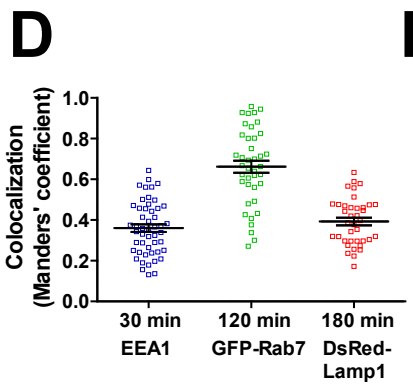
D
Colocalization (Manders' coefficient)
1.0
0.8
0.6
0.4
0.2
0.0
30 min EEA1
120 min GFP-Rab7
180 min DsRed-Lamp1

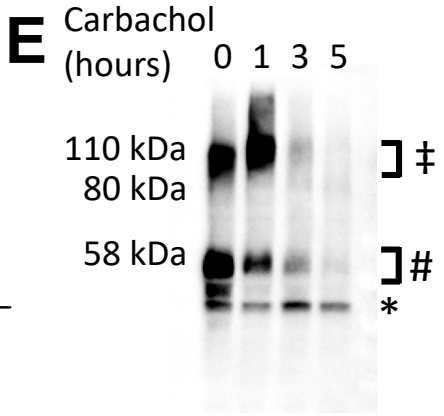
E
Carbachol (hours)
0 1 3 5
110 kDa
80 kDa
58 kDa
‡
#
*

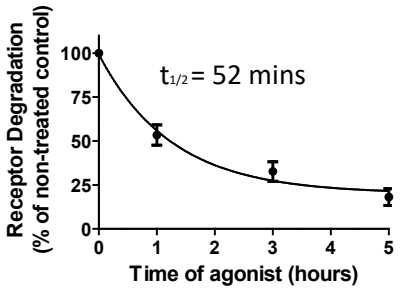
F
Receptor Degradation (% of non-treated control)
100
75
50
25
0
t1/2 = 52 mins
0 1 2 3 4 5
Time of agonist (hours)

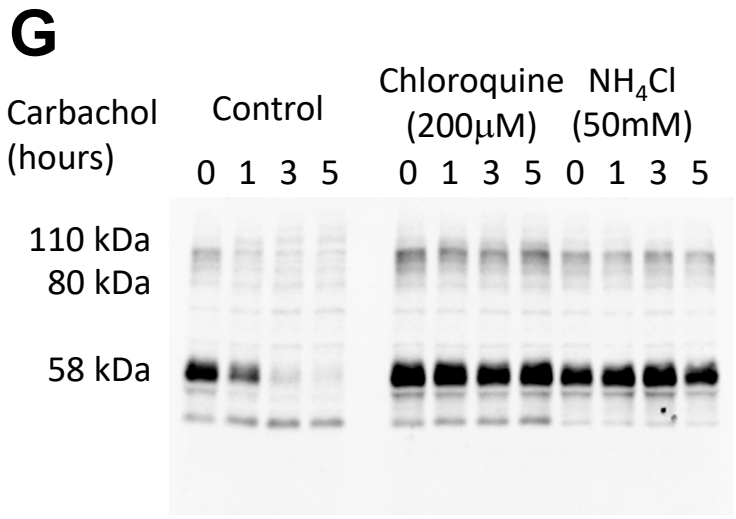
G
Carbachol (hours)
Control
Chloroquine (200µM)
NH4Cl (50mM)
0 1 3 5 0 1 3 5 0 1 3 5
110 kDa
80 kDa
58 kDa

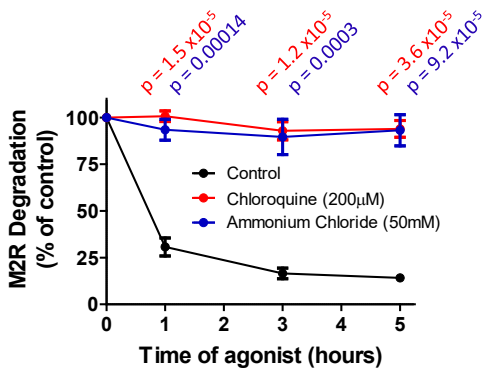
H
p = 1.5 x10-5
p = 0.00014
p = 1.2 x10-5
p = 0.0003
p = 3.6 x10-5
p = 9.2 x10-5
M2R Degradation (% of control)
100
75
50
25
0
Control
Chloroquine (200µM)
Ammonium Chloride (50mM)
0 1 2 3 4 5
Time of agonist (hours)

Figure 2

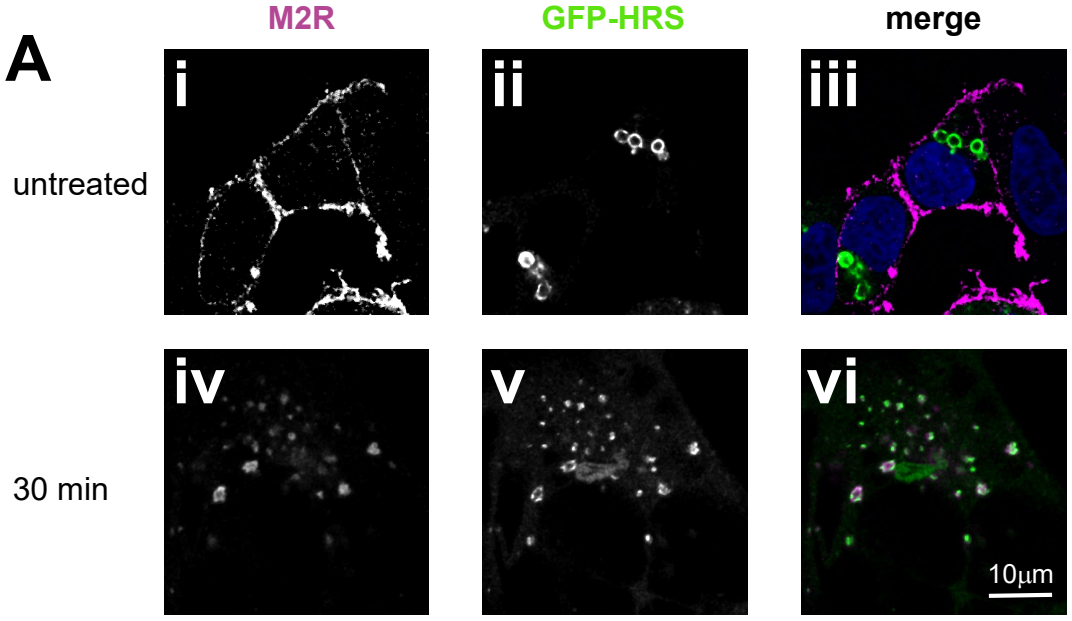
A
M2R
GFP-HRS
merge
untreated
30 min
i
ii
iii
iv
v
vi
10μm

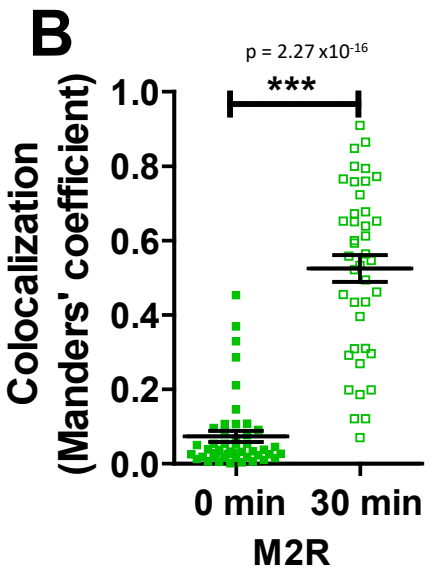
B
p = 2.27 x10-16
***
Colocalization (Manders' coefficient)
1.0
0.8
0.6
0.4
0.2
0.0
0 min
30 min
M2R

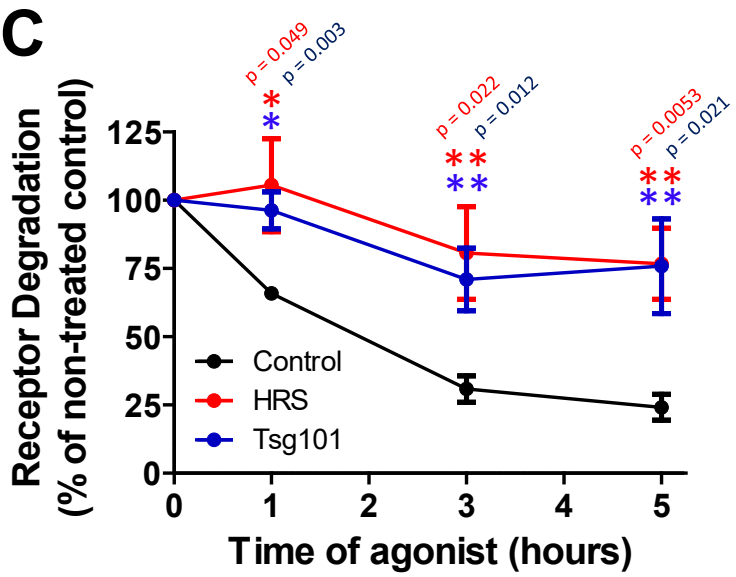
C
p = 0.049
p = 0.003
p = 0.022
p = 0.012
p = 0.0053
p = 0.021
Receptor Degradation (% of non-treated control)
125
100
75
50
25
0
Control
HRS
Tsg101
0
1
2
3
4
5
Time of agonist (hours)

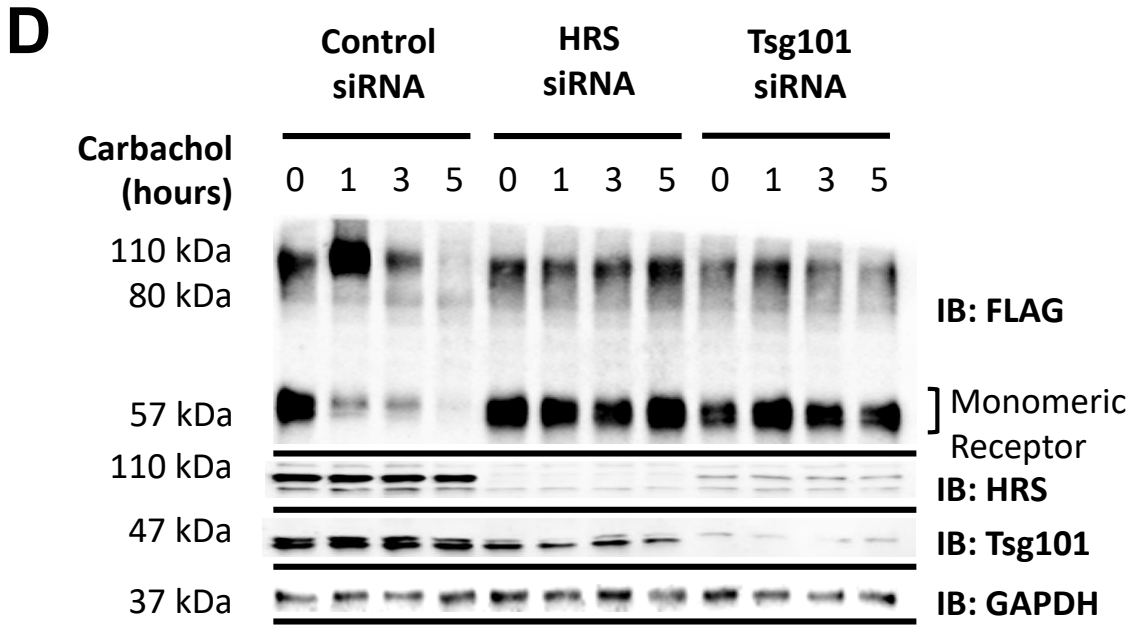
D
Control siRNA
HRS siRNA
Tsg101 siRNA
Carbachol (hours)
0 1 3 5 0 1 3 5 0 1 3 5
110 kDa
80 kDa
57 kDa
110 kDa
47 kDa
37 kDa
IB: FLAG
Monomeric Receptor
IB: HRS
IB: Tsg101
IB: GAPDH

Figure 3

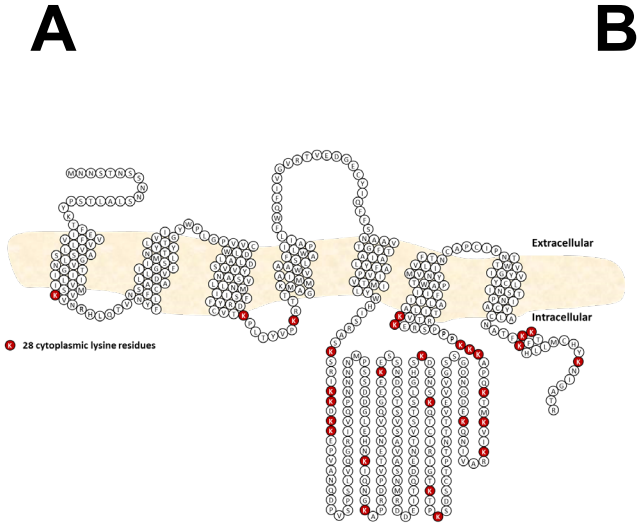
A
Extracellular
Intracellular
28 cytoplasmic lysine residues

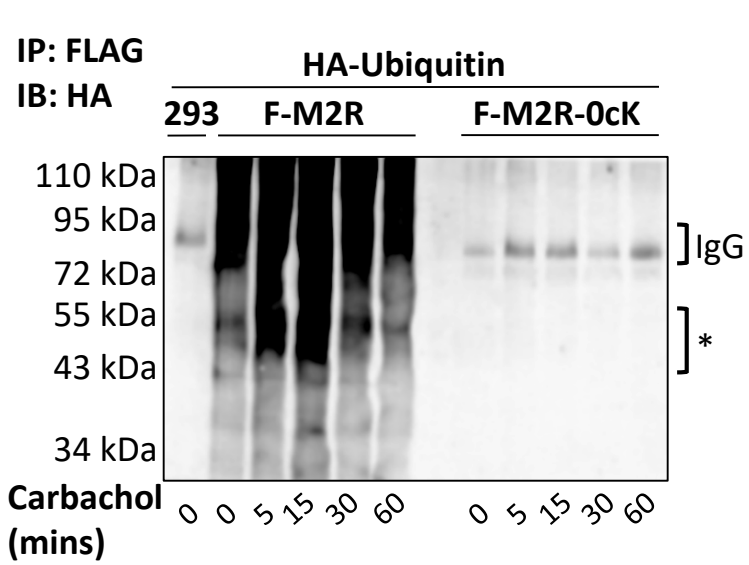
B
IP: FLAG
IB: HA
HA-Ubiquitin
293
F-M2R
F-M2R-0cK
110 kDa
95 kDa
72 kDa
55 kDa
43 kDa
34 kDa
IgG
*
Carbachol (mins)
0 0 5 15 30 60 0 5 15 30 60

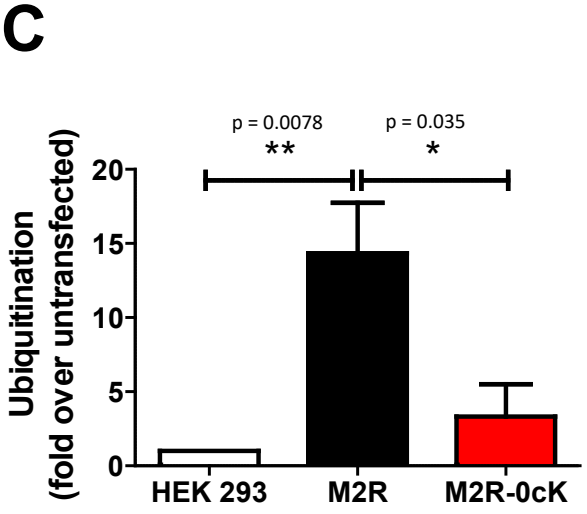
C
p = 0.0078
**
p = 0.035
*
Ubiquitination (fold over untransfected)
20
15
10
5
0
HEK 293
M2R
M2R-0cK

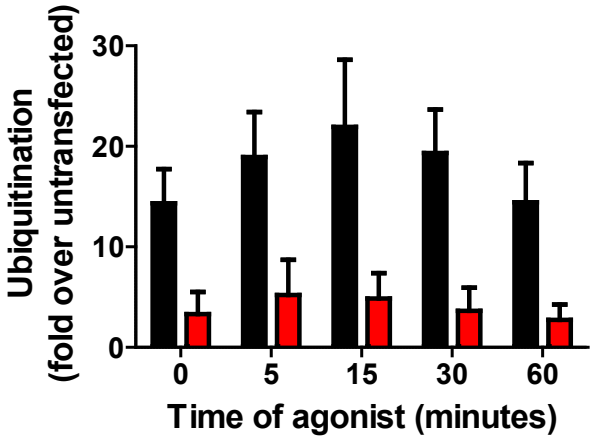
D
Ubiquitination (fold over untransfected)
30
20
10
0
0 5 15 30 60
Time of agonist (minutes)

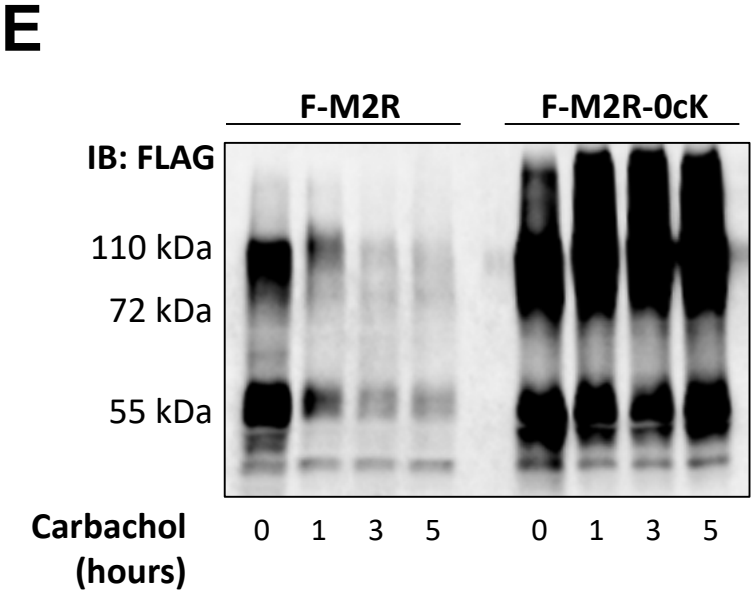
E
F-M2R
F-M2R-0cK
IB: FLAG
110 kDa
72 kDa
55 kDa
Carbachol (hours)
0 1 3 5 0 1 3 5

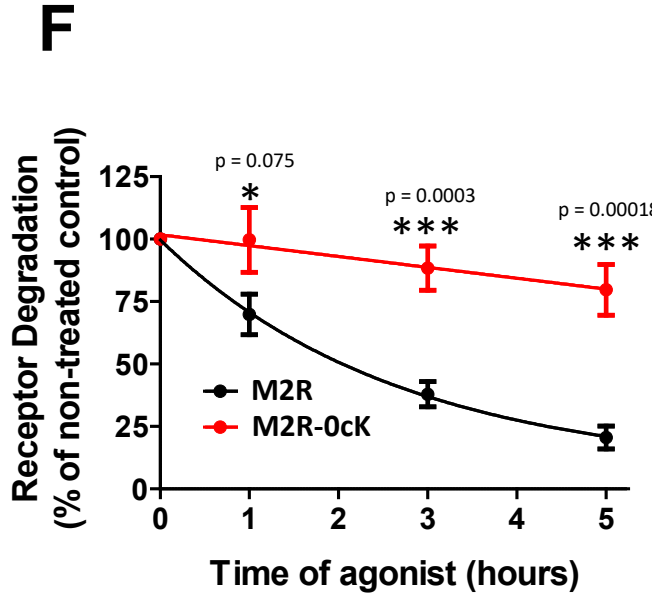
F
p = 0.075
*
p = 0.0003
***
p = 0.00018
***
Receptor Degradation (% of non-treated control)
125
100
75
50
25
0
M2R
M2R-0cK
0 1 2 3 4 5
Time of agonist (hours)

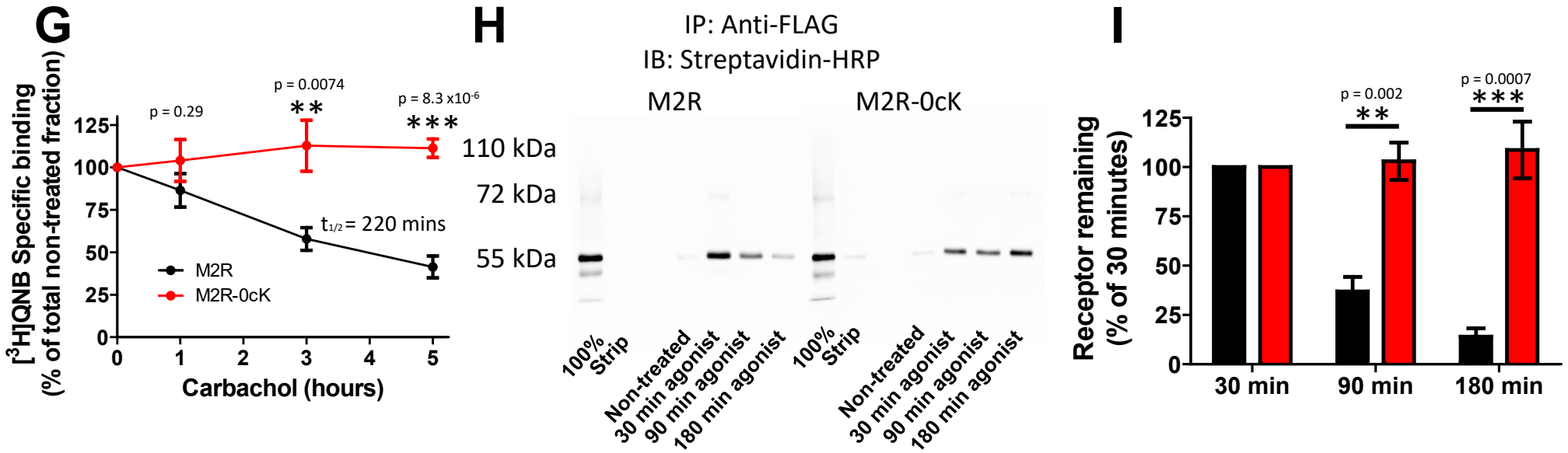
G
[3H]QNB Specific binding
(% of total non-treated fraction)
p = 0.29
p = 0.0074
**
p = 8.3 x10-6
***
t1/2 = 220 mins
M2R
M2R-0cK
Carbachol (hours)
H
IP: Anti-FLAG
IB: Streptavidin-HRP
M2R
M2R-0cK
110 kDa
72 kDa
55 kDa
100% Strip
Non-treated
30 min agonist
90 min agonist
180 min agonist
I
Receptor remaining
(% of 30 minutes)
p = 0.002
**
p = 0.0007
***
30 min
90 min
180 min

Figure 4

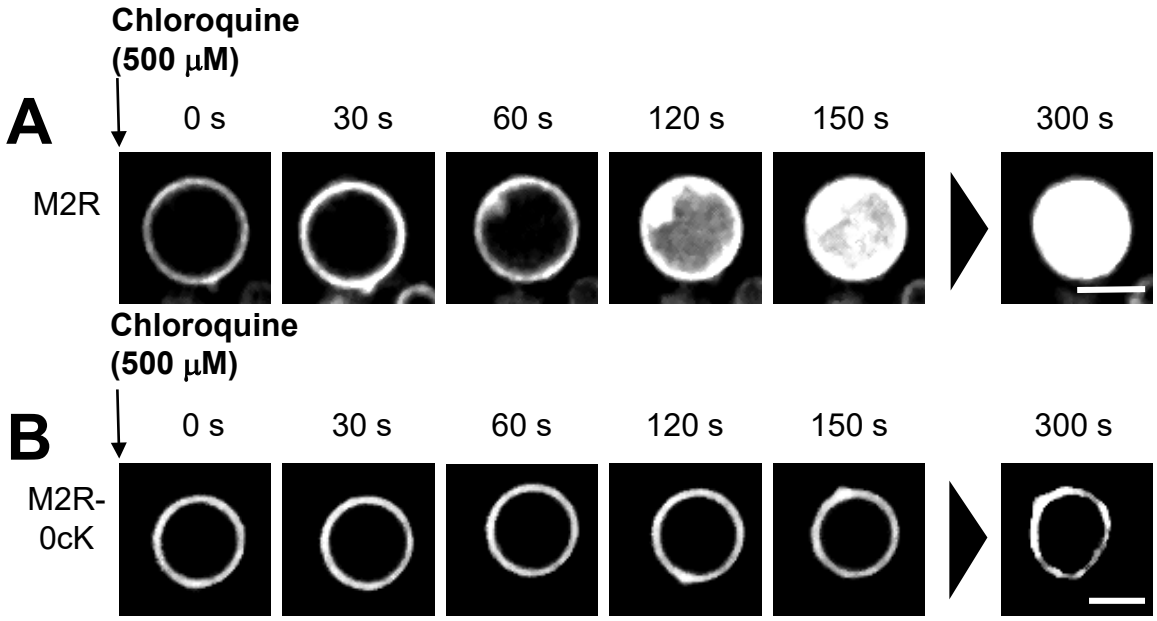
Chloroquine
(500 μM)
A
0 s
30 s
60 s
120 s
150 s
300 s
M2R
Chloroquine
(500 μM)
B
0 s
30 s
60 s
120 s
150 s
300 s
M2R-
0cK

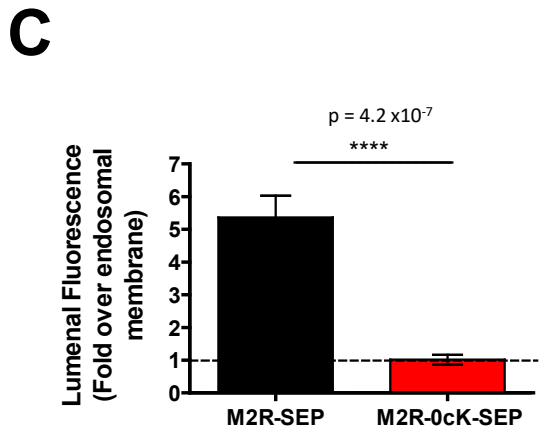
C
p = 4.2 x10-7
****
Lumenal Fluorescence
(Fold over endosomal
membrane)
7
6
5
4
3
2
1
0
M2R-SEP
M2R-0cK-SEP

Figure 5

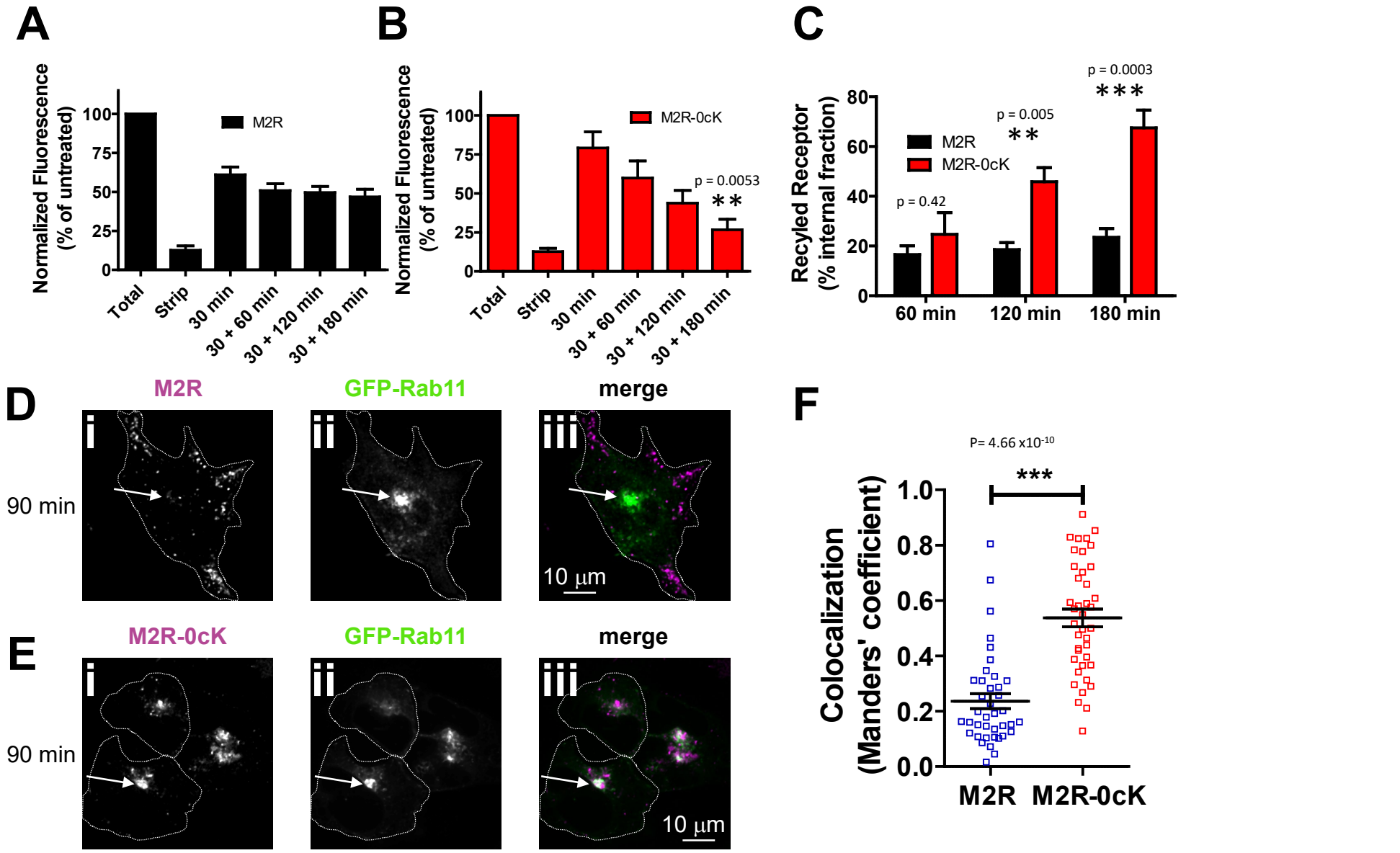
A
Normalized Fluorescence (% of untreated)
M2R
Total
Strip
30 min
30 + 60 min
30 + 120 min
30 + 180 min
B
Normalized Fluorescence (% of untreated)
M2R-0cK
p = 0.0053
**
C
Recyled Receptor (% internal fraction)
M2R
M2R-0cK
p = 0.42
p = 0.005
**
p = 0.0003
***
60 min
120 min
180 min
D
M2R
GFP-Rab11
merge
90 min
i
ii
iii
10 μm
E
M2R-0cK
GFP-Rab11
merge
90 min
10 μm
F
P= 4.66 x10-10
***
Colocalization (Manders' coefficient)
M2R
M2R-0cK

Figure 6

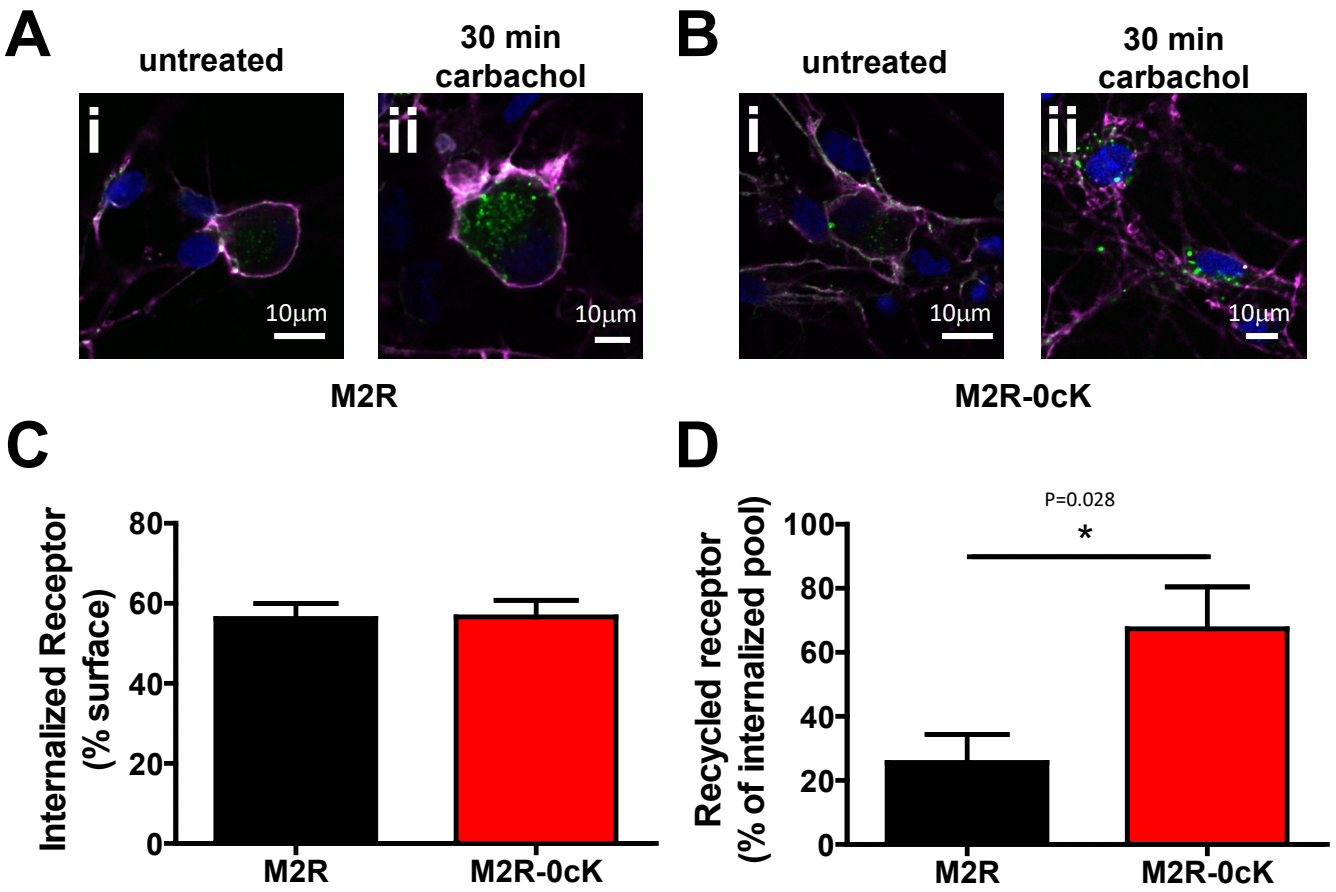
A
untreated
30 min carbachol
i
ii
10μm
10μm
M2R
B
untreated
30 min carbachol
i
ii
10μm
10μm
M2R-0cK
C
Internalized Receptor (% surface)
80
60
40
20
0
M2R
M2R-0cK
D
Recycled receptor (% of internalized pool)
P=0.028
*
100
80
60
40
20
0
M2R
M2R-0cK

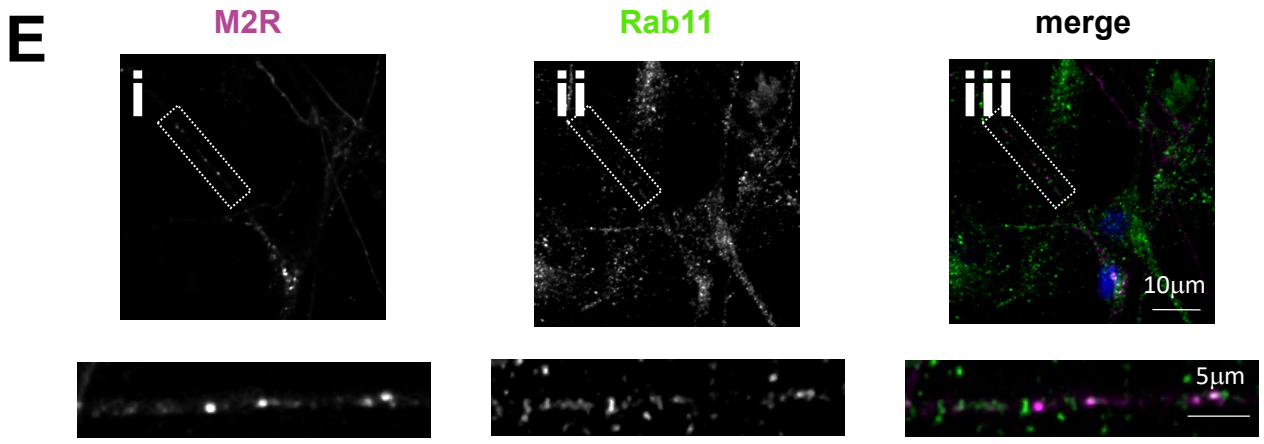
E
M2R
Rab11
merge
i
ii
iii
10μm
5μm

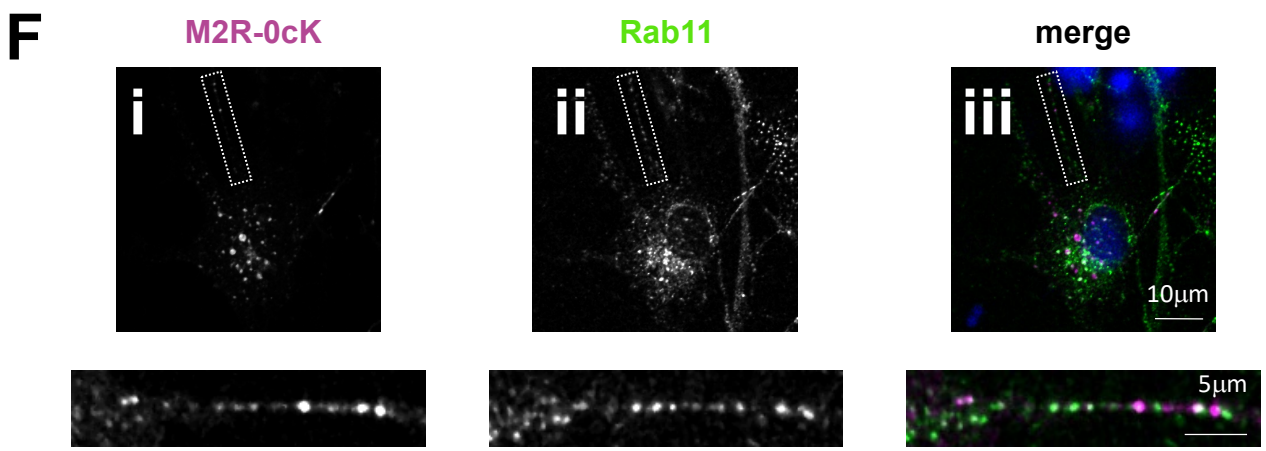
F
M2R-0cK
Rab11
merge
i
ii
iii
10μm
5μm

Supplemental Figure Legends

Supplemental Figure 1 – Analysis of M2R colocalization.

A-C) Shows the untreated conditions corresponding to Figure 1. HEK 293 cells were transiently transfected with N terminally Flag-tagged M2R (M2R) alone (A) or with the indicated marker (B and C) and plated on coverslips. Cells were incubated with AF-M1 antibody (magenta, i) for 60 mins before fixing. A) M2R-AF568 (magenta, i) and cells stained with anti-EEA1 (green, ii). B) M2R-AF-568 (magenta, i) and GFP-Rab7 (green, ii). C) M2R-AF488 (magenta, i) and DsRed-LAMP1 (green, ii). Dotted lines show the outline of the cells. D) Quantification of colocalization by Manders' coefficient and statistical analysis using unpaired t-test with Welch correction for unequal variance, between untreated (0) and carbachol treated conditions. EEA1 – $t(55)=17.02$, $p=1.03 \times 10^{-23}$, GFP-Rab7 – $t(57)=15.16$, $p=1.08 \times 10^{-21}$, DsRed-LAMP1 – $t(50) = 15.07$, $p=2.27 \times 10^{-20}$.

Supplemental Figure 2 – Characterization of M2R-0cK

A-C) HEK 293 cells were transiently transfected with N-terminally Flag-tagged M2R-0cK and the indicated marker and plated on coverslips. Cells were incubated at 37°C with AF-labelled M1 anti-Flag, for 30 minutes before agonist treatment with 1 μM carbachol for the indicated times before fixation. A) M2R-0cK-AF568 (magenta, i and iv) and cells stained with anti-EEA1 (green, ii and v). B) M2R-0cK-AF568 (magenta, i and iv) and GFP-Rab7 (green, ii and v). C) M2R-0cK-AF488 (magenta, i and iv) and Ds-Red-LAMP1) (green, ii and v). Dotted lines show the outline of the cell. D) HEK293 cells were transiently transfected with F-M2R or F-M2R-0cK and incubated with anti-Flag-AF647 for 30 mins before addition of 1μM carbachol for the indicated time. Cells were then washed and incubated in PBS/EDTA to remove any antibody bound to surface receptor, and remaining fluorescence measured by flow cytometry. Internalization between receptors was unchanged (mean ± SEM, n=4. Two-Way ANOVA: $F(3,24)=0.153$, $p=0.927$). E) DREADD mutations (Y104C, A193G) were introduced into the M2R and M2R-0cK as designed by Armbruster et al., 2007. Stable cell lines expressing the receptors were then treated for 7 minutes with the indicated concentration of Clozapine-N-oxide, before lysis and analysis by SDS-PAGE, and probed for phospho-ERK. Shown is a representative immunoblot (n=2), indicating no difference in the signalling of the 'WT' or 0cK receptors. F) Quantification of

colocalization by Manders' coefficient, and comparison with similarly treated cells expressing M2R as described in Figure 1, using unpaired t-test. Colocalization of M2R (50 cells) or M2R-0cK (32 cells) with EEA1 after 30 mins carbachol – $t(79)=3.18$, $p=0.004$. Colocalization of M2R (40 cells) or M2R-0cK (43 cells) with GFP-Rab7 after 120 mins carbachol – $t(81)=5.864$, $p=9.4x10^{-8}$. Colocalization of M2R (38 cells) or M2R-0cK (38 cells) with DsRed-LAMP1 after 180 mins carbachol – $t(69)=5.995$, $p=2.7x10^{-5}$.

Supplemental Figure 3 – lysine mutation prevents involution of the M2R.

Schematic of assay and quantification as previously described (Henry et al., 2011). HEK 293 cells were transiently transfected with mCherry-Rab5-Q79L and ether F-M2R-SEP (B) or F-M2R-0cK-SEP (C) and plated on coverslips. Cells were then treated with carbachol (10μM) for 90 mins before imaging by spinning disc confocal microscopy. Cells were imaged for 1 minute and then 500 μM chloroquine was added, and the cells imaged for a further 5 minutes. Shown is a representative image series (four independent experiments) of the whole cell, and the enlarged endosome inset, showing the increase in intraluminal fluorescence, for M2R (B) and M2R-0cK (C). The chloroquine induced fluorescence was then quantified by taking the mean fluorescence of the endosome immediately after chloroquine addition (6 frames) and after 5 mins (6 frames) and expressed as a fold increase.

Supplemental Figure 4 – Surface expression is unchanged by coexpression of GFP-Rab11.

HEK293 cells were transfected with GFP-Rab11 and either M2R or M2R-0cK, and then plated onto coverslips. Cells were incubated with AF568 labelled M1 anti-Flag for 60 minutes at 37°C, before fixation and mounting for confocal analysis.

Supplemental Figure 5 – Ratiometric internalization of M2R in DRG cells

DRG cultures transfected with F-M2R were fed with anti-FLAG-M1-AF-488 (green) and left either untreated (i) or treated for 30 minutes with 1 μM carbachol (iii). Cells were then fixed with 4% paraformaldehyde under non-permeabilising conditions, and then incubated with anti-mouse secondary conjugated to AF594, which only label antibody still on the surface of the cell (ii and iv). The ratio of 488 to 594 fluorescence was then measured by fluorescent microscopy for each condition, and then the ratio

measured in the agonist treated condition expressed as a percentage of the ratio in the untreated condition to give the internalized fraction (Yu et al., 2010).

Supplemental Figure 6

A-C) Original and uncropped anti-Flag Western blots corresponding to Figure 1E (first four lanes on left side) and 1G

Supplemental Figure 7

A-D) Original and uncropped Western blots corresponding to Figure 2D. A) is the anti-Flag blot, B) anti-HRS, C) anti-Tsg101 and D) is anti-GAPDH

Supplemental Figure 8

A-D) Original and uncropped Western blots corresponding to Figure 3. A) is the anti-HA blot corresponding to Figure 3B. B) is the anti-Flag blot of Figure 3E. C and D) are the biotin-streptavidin blots of Figure 3H. C shows M2R and D shows M2R-0cK

Supplemental Figure 1

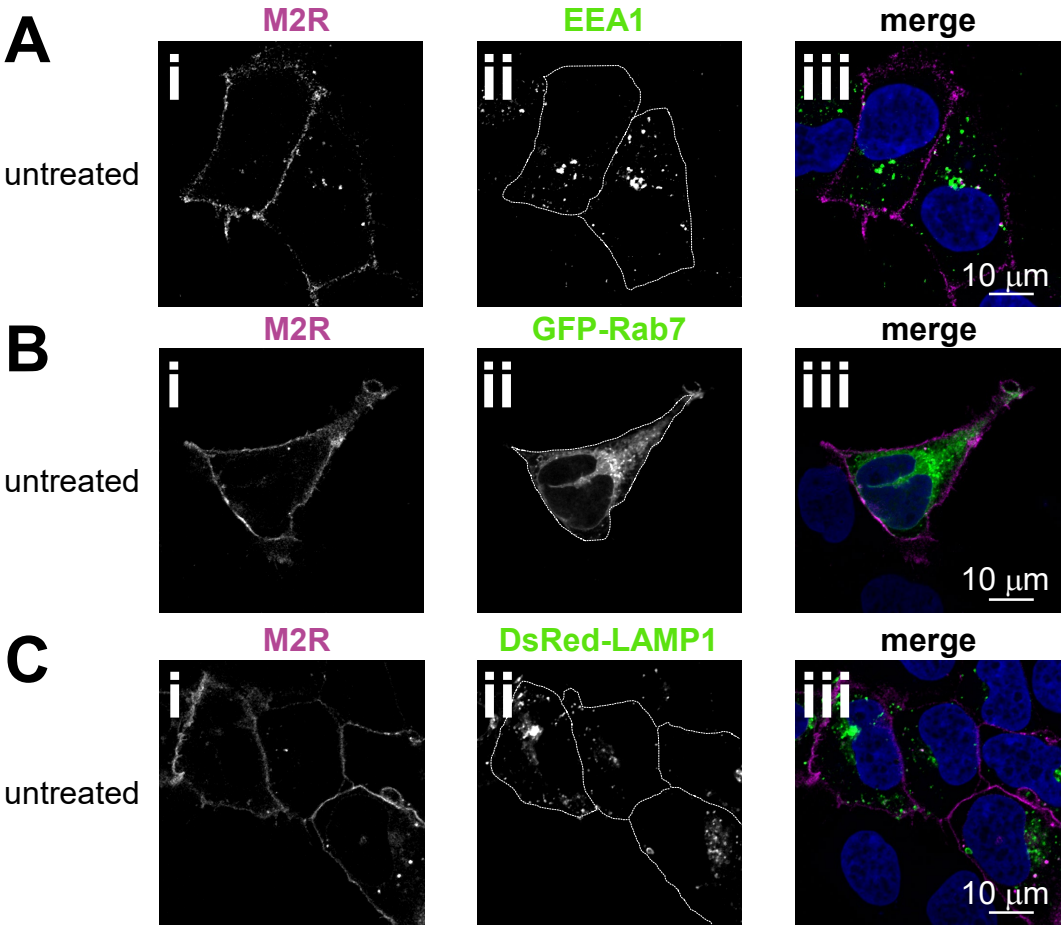

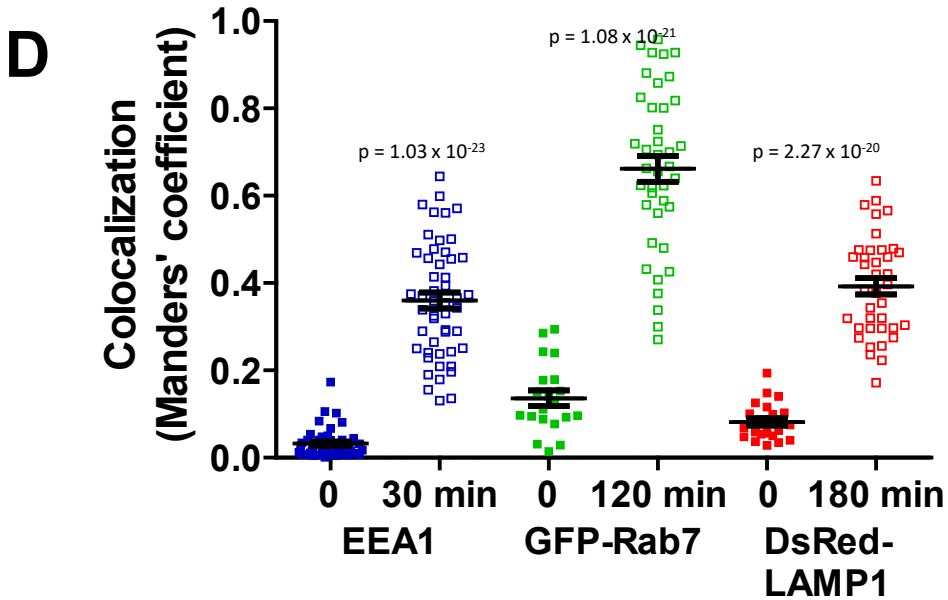

Supplemental Figure 2

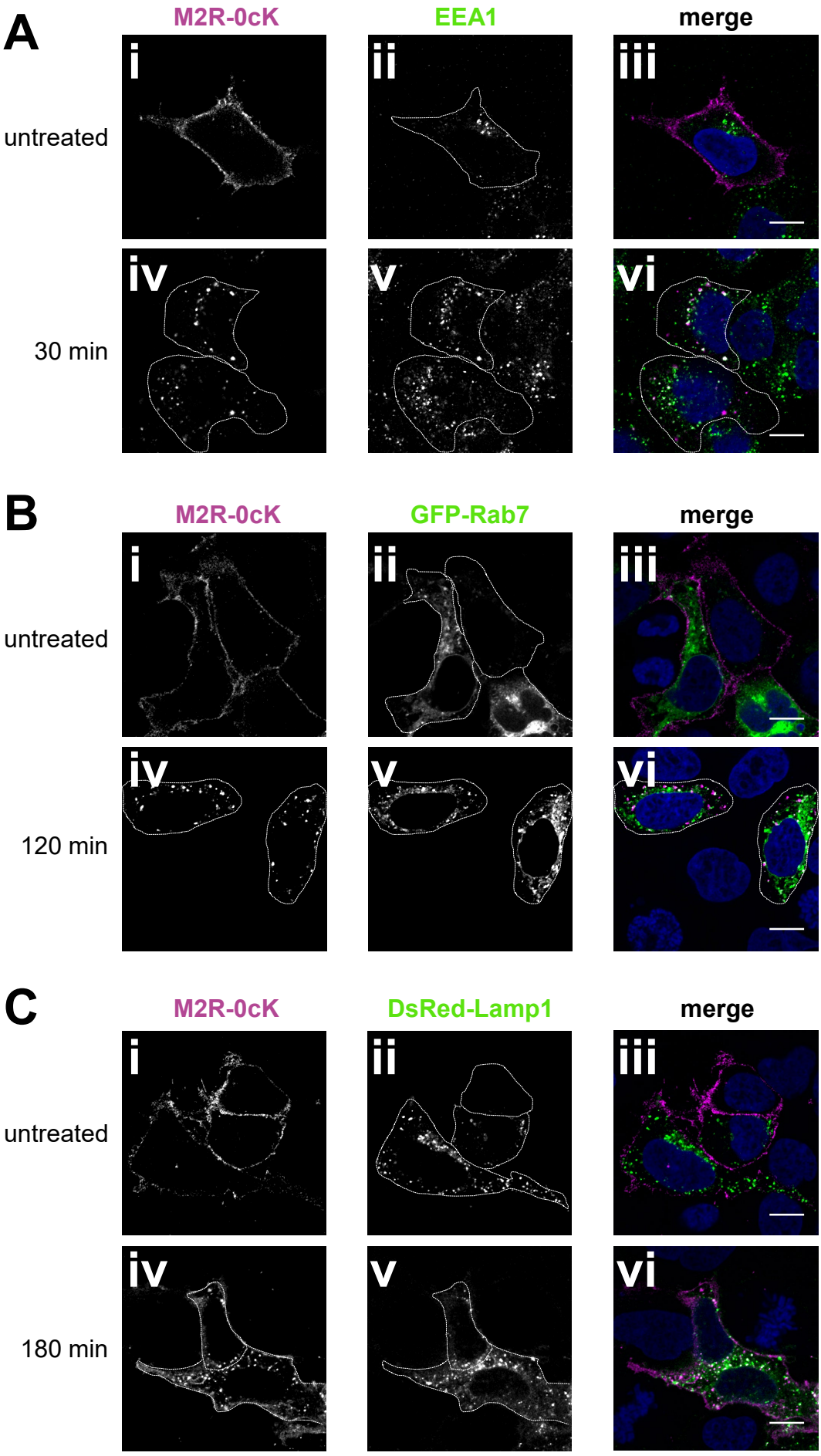

D

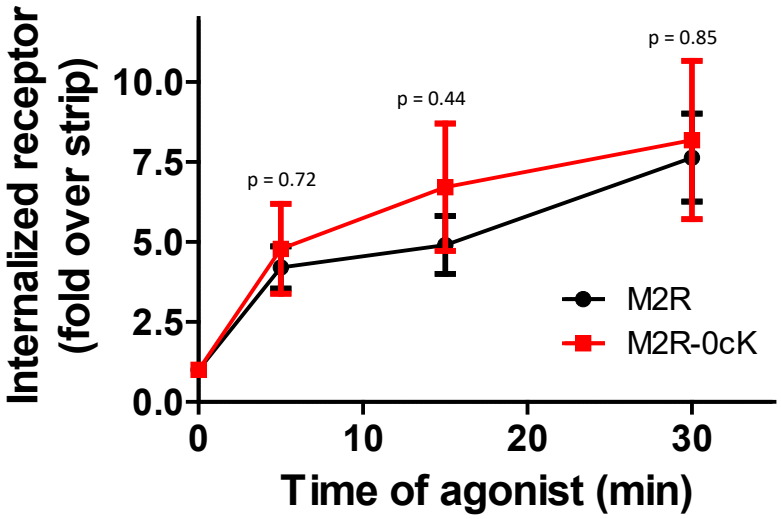
Internalized receptor (fold over strip)
10.0
7.5
5.0
2.5
0.0
0
10
20
30
Time of agonist (min)
p = 0.72
p = 0.44
p = 0.85
M2R
M2R-0cK

E

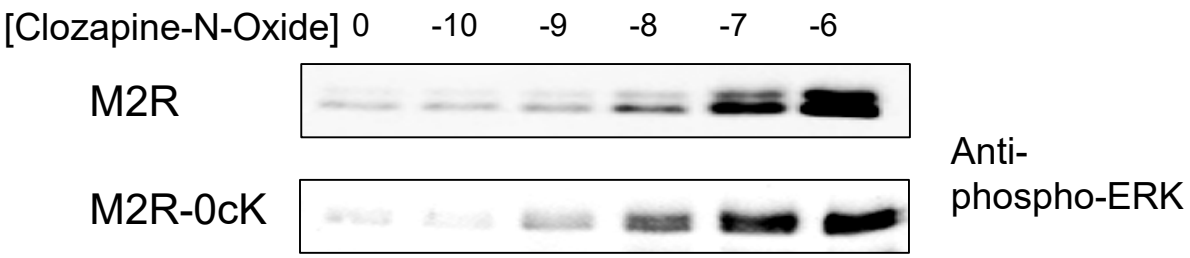
[Clozapine-N-Oxide] 0
-10
-9
-8
-7
-6
M2R
M2R-0cK
Anti-
phospho-ERK

F

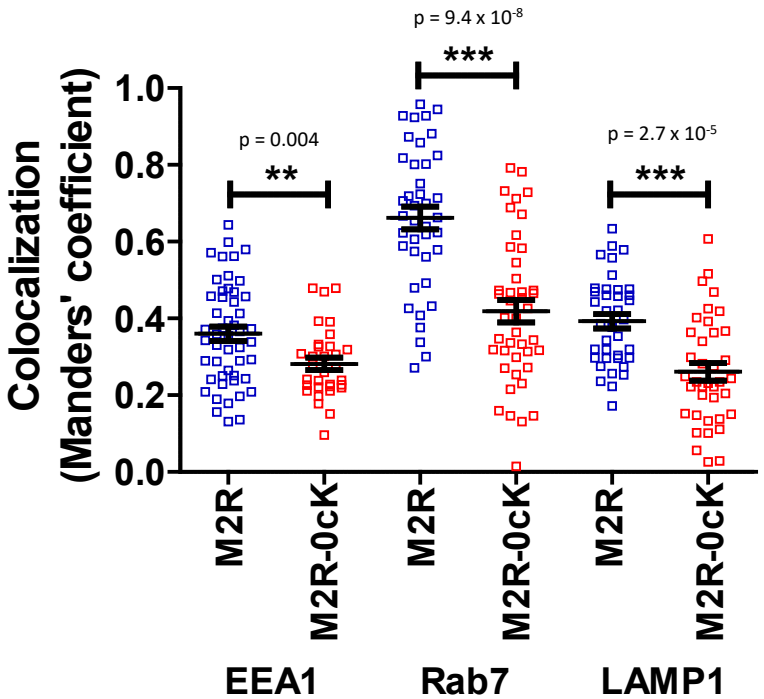
Colocalization (Manders' coefficient)
1.0
0.8
0.6
0.4
0.2
0.0
p = 0.004
**
p = 9.4 x 10-8
***
p = 2.7 x 10-5
***
M2R
M2R-0cK
M2R
M2R-0cK
M2R
M2R-0cK
EEA1
Rab7
LAMP1

Supplemental Figure 3

A

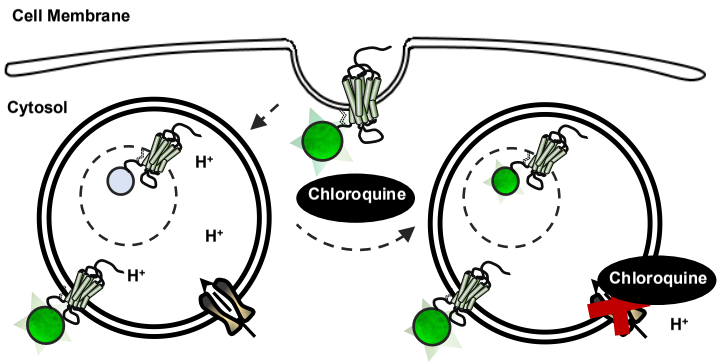

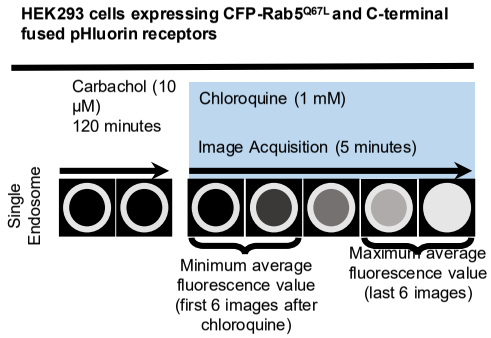

B

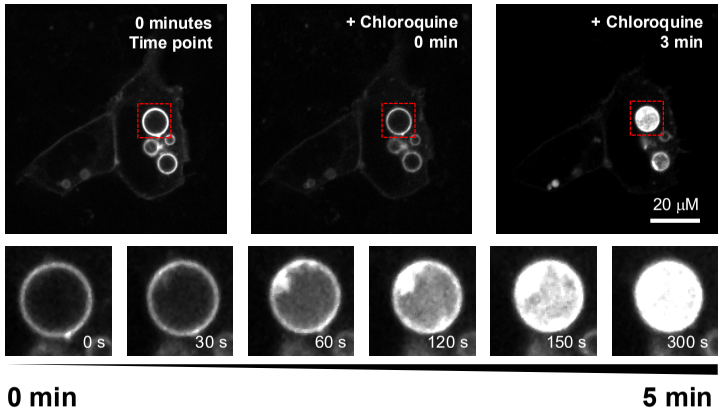

C

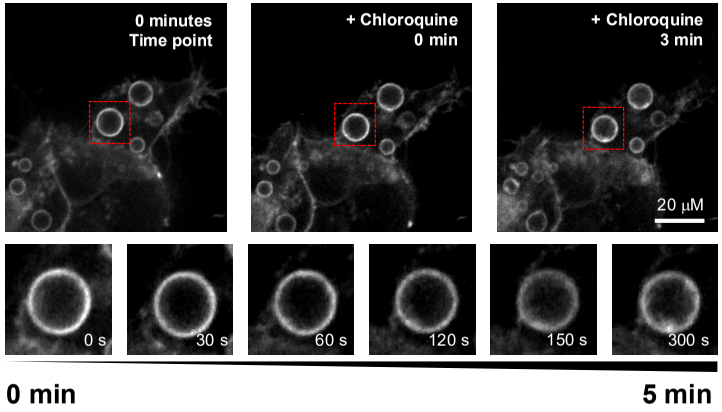

Supplemental Figure 4

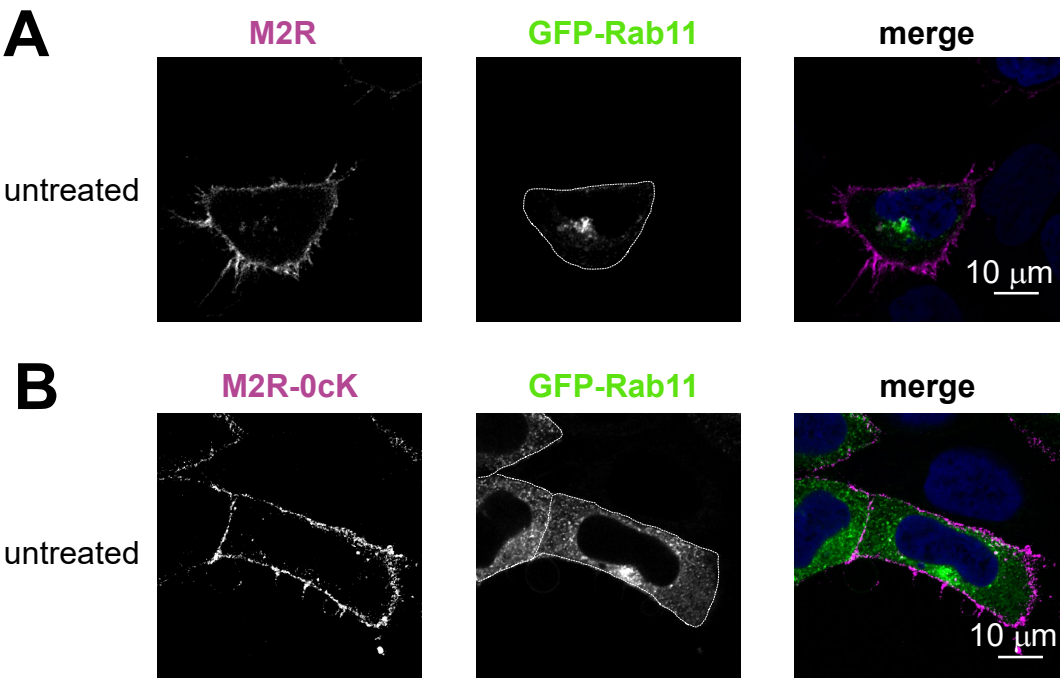

Supplemental Figure 5

Untreated

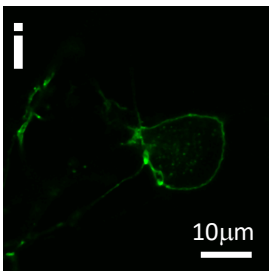

Anti-Flag
(AF488)

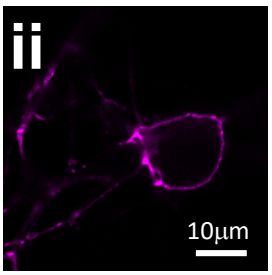

Anti-Mouse
(AF594)

$$\frac{\text{Fluorescence in (i)}}{\text{Fluorescence in (ii)}} = \text{Total}$$

30 min Agonist

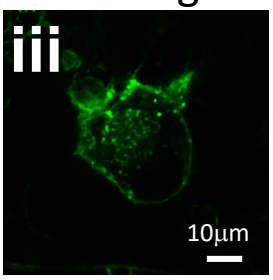

Anti-Flag
(AF488)

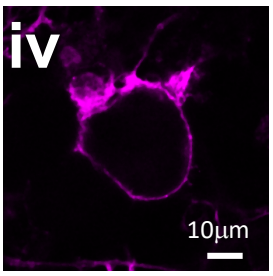

Anti-Mouse
(AF594)

$$\frac{\text{Fluorescence in (iii)}}{\text{Fluorescence in (iv)}} = \text{Internal}$$

$$\left(\frac{\text{Internal}}{\text{Total}}\right) \times 100 = \text{Internalization (\%)}$$

Supplemental Figure 6

A

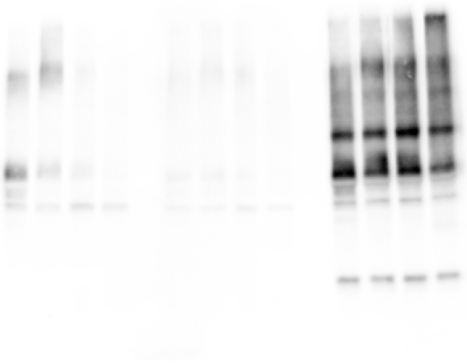

B

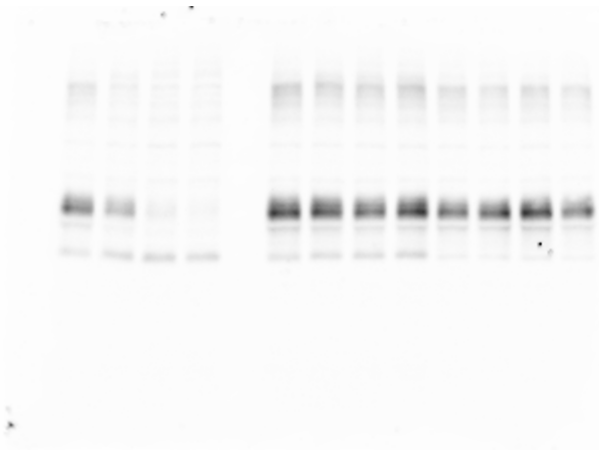

Supplemental Figure 7

A

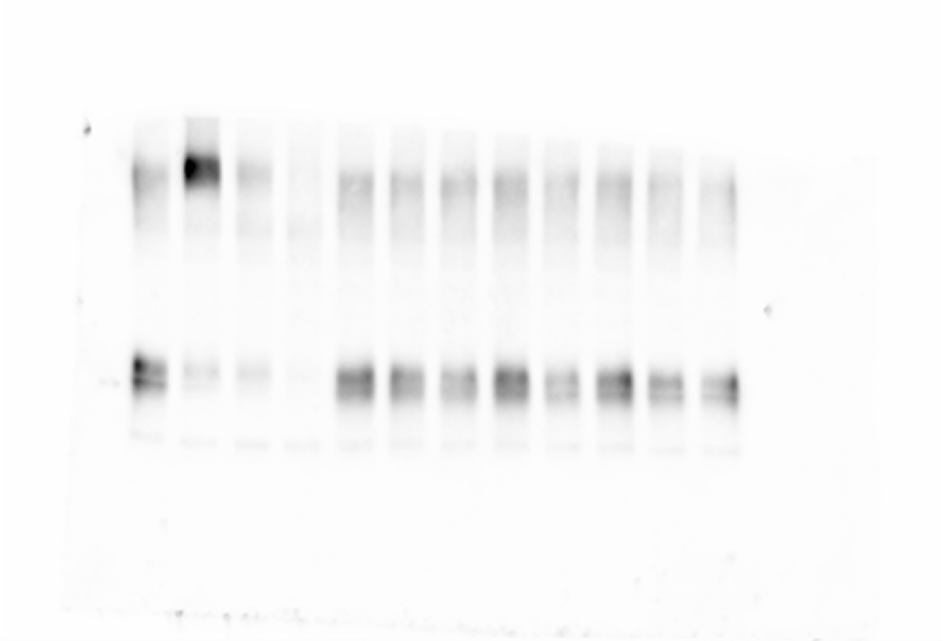

B

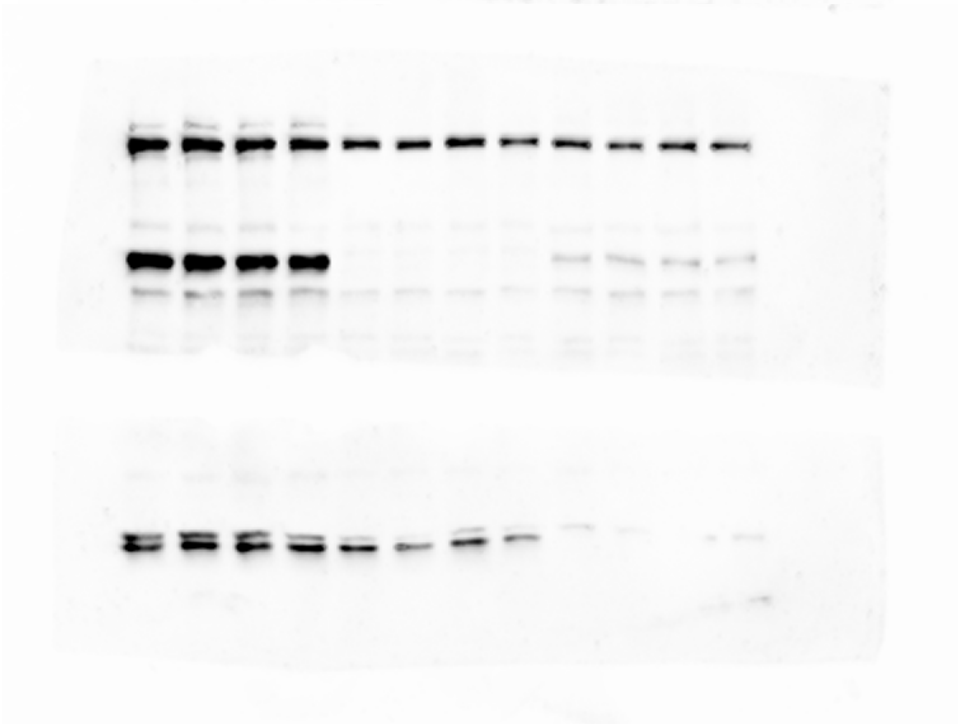

C

D

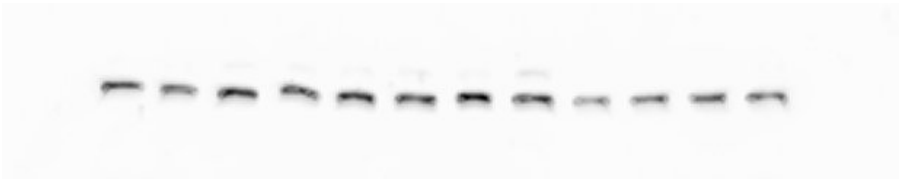

Supplemental Figure 8

A

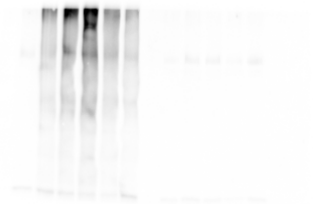

B

C

D